TREATMENT WITH SOLUBLE CD24 ATTENUATES COVID-19-ASSOCIATED SYSTEMIC IMMUNOPATHOLOGY

No-Joon Song, Ph.D.[3], Carter Allen[1,3,4], Anna E. Vilgelm, M.D., Ph.D.[3,6,10], Brian P. Riesenberg, Ph.D.[3], Kevin P. Weller[3], Kelsi Reynolds[3], Karthik B. Chakravarthy, B.S.[3,11], Amrendra Kumar, Ph.D.[6,10], Aastha Khatiwada, M.S.[5], Zequn Sun, M.S.[5], Anjun Ma, Ph.D.[4], Yuzhou Chang[1,3,4], Mohamed Yusuf[6], Anqi Li[1,3,11], Cong Zeng, Ph.D.[12], John P. Evans[12], Donna Bucci[3], Manuja Gunasena, Ph.D.[8,9], Menglin Xu, Ph.D.[2], Namal P.M. Liyanage, Ph.D.[8,9], Chelsea Bolyard, Ph.D.[3], Maria Velegraki, M.D., Ph.D.[3], Shan-Lu Liu, M.D., Ph.D.[12], Qin Ma, Ph.D.[4], Martin Devenport, Ph.D., M.B.A.[13], Yang Liu, Ph.D.[13], Pan Zheng, M.D., Ph.D.[13], Carlos D. Malvestutto, M.D., M.P.H.[2], Dongjun Chung, Ph.D.[3,4], and Zihai Li, M.D., Ph.D.[2,3]

Full Affiliations:

[1]The Ohio State University, Columbus, OH, USA
[2]Department of Internal Medicine, The Ohio State University College of Medicine, Columbus, OH
[3]The Pelotonia Institute for Immuno-Oncology, The Ohio State University Comprehensive Cancer Center, Columbus, OH, USA
[4]Dept of Biomedical Informatics, The Ohio State University College of Medicine, Columbus, OH
[5]Department of Public Health Sciences, Medical University of South Carolina, Charleston, SC
[6]The Ohio State University Comprehensive Cancer Center, Columbus, OH
[7]Department of Microbiology, The Ohio State University College of Arts and Sciences, Columbus, OH, USA
[8]Department of Microbial Infection and Immunity, The Ohio State University College of Medicine, Columbus, OH, USA
[9]Department of Veterinary Biosciences, The Ohio State University College of Veterinary Medicine, Columbus, OH, USA
[10]Department of Pathology, The Ohio State University College of Medicine, Columbus, OH
[11]The Ohio State University College of Medicine, Columbus, OH, USA
[12]Center for Retrovirus Research and Department of Veterinary Biosciences, The Ohio State University, Columbus, OH, USA
[13]OncoC4, Rockwille, MD, USA

N-J.S., C.A., A.V. and B.P.R. are co-first authors. C.D.M., D.C. and Z.L. are co-senior authors.

Address reprint requests to Dr. Zihai Li (corresponding author), Pelotonia Institute for Immuno-Oncology, The Ohio State University James Comprehensive Cancer Center, Columbus, Ohio 43210, USA, or zihai.li@osumc.edu.

ABSTRACT

BACKGROUND. SARS-CoV-2 causes COVID-19 through direct lysis of infected lung epithelial cells, which releases damage-associated molecular patterns (DAMPs) and induces a pro-inflammatory cytokine milieu causing systemic inflammation. Anti-viral and anti-inflammatory agents have shown limited therapeutic efficacy. Soluble CD24 (CD24Fc) is able to blunt the broad inflammatory response induced by DAMPs in multiple models. A recent randomized phase III trial evaluating the impact of CD24Fc in patients with severe COVID-19 demonstrated encouraging clinical efficacy.

METHODS. We studied peripheral blood samples obtained from patients enrolled at a single institution in the SAC-COVID trial (NCT04317040) collected before and after treatment with CD24Fc or placebo. We performed high dimensional spectral flow cytometry analysis of peripheral blood mononuclear cells and measured the levels of a broad array of cytokines and chemokines. A systems analytical approach was used to discern the impact of CD24Fc treatment on immune homeostasis in patients with COVID-19.

FINDINGS. Twenty-two patients were enrolled, and the clinical characteristics from the CD24Fc vs. placebo groups were matched. Using high-content spectral flow cytometry and network-level analysis, we found systemic hyper-activation of multiple cellular compartments in the placebo group, including $CD8^+$ T cells, $CD4^+$ T cells, and $CD56^+$ NK cells. By contrast, CD24Fc-treated patients demonstrated blunted systemic inflammation, with a return to homeostasis in both NK and T cells within days without compromising the ability of patients to mount an effective anti-Spike protein antibody response. A single dose of CD24Fc significantly attenuated induction of the systemic cytokine response, including expression of IL-10 and IL-15, and diminished the coexpression and network connectivity among extensive circulating inflammatory cytokines, the parameters associated with COVID-19 disease severity.

INTERPRETATION. Our data demonstrates that CD24Fc treatment rapidly down-modulates systemic inflammation and restores immune homeostasis in SARS-CoV-2-infected individuals, supporting further development of CD24Fc as a novel therapeutic against severe COVID-19.

FUNDING. NIH

INTRODUCTION

The pathogenesis of SARS-CoV-2 is a multistep process starting with the infection of ACE2-expressing lung epithelial cells[1]. Following infection, unconstrained viral replication leads to cell lysis and the release of DAMPs. Recognition of these molecules by neighboring cells produces a pro-inflammatory milieu through the release of cytokines (such as IL-6 and IL-10), which recruit and activate monocytes, macrophages, and T cells[2]. In severe COVID-19, this pro-inflammatory feedback loop results in a persistent and harmful response that leads to structural damage of the lung. The resulting cytokine storm can lead to acute respiratory distress syndrome (ARDS), multi-organ failure and death[3].

Even though COVID-19 mRNA vaccines have shown great success in preventing severe disease[4], recent reports suggest that new SARS-CoV-2 variant delta can escape from the immune response induced by existing vaccines[5]. Breakthrough infections post full vaccinations can occur[6], especially in immunocompromized individuals[7], requiring urgent development of effective therapeutic agents against this disease. Interim results from the Solidarity trial (NCT04315948) indicate that several repurposed interventions do not significantly alter COVID-19 morbidity and mortality[8]. Other approaches, including cytokines and convalescent plasma, have also been largely ineffective[9,10]. The anti-inflammatory glucocorticoid dexamethasone is one of the few interventions shown to reduce mortality in patients with critical-to-severe COVID-19[11].

CD24Fc treatment attenuates inflammation associated with viral infections, autoimmunity, and graft-versus-host diseases[12-14]. In this study, we compared blood samples from COVID-19 patients enrolled in the SAC-COVID trial following CD24Fc or placebo. We examined dynamic changes in peripheral blood mononuclear cells (PBMCs) and systemic cytokine and chemokine levels. We demonstrated that CD24Fc reversed the inflammatory hallmarks associated with severe COVID-19, including cytokine storm and immune hyperactivation.

METHODS

PATIENTS AND TRIAL PROCEDURE. This study included samples from patients enrolled in NCT04317040 at The Ohio State University Wexner Medical Center (patient details described in **Table S1**). Patients eligible for this trial were hospitalized with COVID-19, requiring supplemental oxygen but not mechanical ventilation, with a prior positive SARS-CoV-2 PCR test. Consented and enrolled patients were randomized in a double-blinded fashion to receive either CD24Fc antibody (480 mg IV infusion) or placebo control (IV saline). Peripheral blood samples were collected from patients before (day 1, D1) and after (D2, D4, D8, D15, and D29) treatment. The Western Institutional Review Board approved trial and protocol. The study was monitored by a contract research organization; safety reports were submitted to an independent Data and Safety Monitoring Board. This trial was conducted in compliance with the protocol, International Conference on Harmonization Good Clinical Practice, and all applicable regulatory requirements.

LABORATORY ASSAYS. Immune profiling, viral neutralization, and cytokine/chemokine assays were performed at The Ohio State University, and per manufacturer's instructions as applicable[15,16]. We developed multiple high dimensional spectral flow cytometry panels to study the dynamic changes of $CD8^+$, $CD4^+$, and $CD56^+$ immune cell subsets (**Table S2**). See Supplementary Appendix for details.

BIOINFORMATICS AND STATISTICAL ANALYSIS. Bioinformatic analyses were performed as previously described[17-25]. Flow cytometry data were preprocessed using the OMIQ software, visualized using the Uniform Manifold Approximation and Projection (UMAP) algorithm, and analyzed using a multivariate t-mixture model[17]. Immune cell activation score was constructed by aggregating pre-selected activation markers[18,19] using a principal component analysis (PCA) applied to the flow cytometry data of

HD and baseline COVID-19 patients. Cytokine score was constructed using a weighted sum approach and validated using PCA and autoencoder approaches[20]. Network-level analysis of cytokine data was implemented by constructing a correlation network between cytokines and evaluating the network structure and importance of each node in the network based on an eigenvector centrality (EC) score[24]. Group comparisons were evaluated using independent sample t-test or Kruskal-Wallis test for continuous variables, and Chi-squared test for categorical variables. Longitudinal analyses were implemented using generalized linear mixed models (GLMMs).

RESULTS

POPULATION DYNAMICS OF IMMUNE CELLS. We utilized a high dimensional spectral flow cytometry panel with an extensive array of immune population markers (**Table S2**) to analyze the systemic effects of SARS-CoV-2 and CD24Fc treatment on PBMCs. Using an unbiased clustering approach based on a multivariate *t*-mixture model[17], we identified 12 distinct clusters that we visualized in two dimensions using the UMAP algorithm (**Fig 1A**). Using clustered heatmap analysis, we correlated expression intensity with clusters to annotate B cells (clusters 1, 6, 8), $CD8^+$ T cells (clusters 7, 11, 12), $CD4^+$ T cells (clusters 2, 3), γδ T cells (cluster 4), NK cells (cluster 10), and myeloid cells (clusters 5, 9) (**Fig 1B**). Comparing systemic immune population dynamics (**Fig 1C-D**), we found significant increases in plasma B cells (cluster 6), NK cells (cluster 10), and terminally differentiated $CD8^+$ T cells (cluster 12) in baseline (D1) COVID-19 patients vs. healthy donors (HD). Conversely, we found that HD samples were enriched for naïve $CD8^+$ T cells (cluster 11) and a subset of myeloid cells (cluster 5). These initial findings were consistent with established immunopathology of SARS-CoV-2 infection and the important role the adaptive immune system plays in viral pathogen response[26-29], and thus validated our experimental approach.

We next used UMAP contour plots to investigate the effects of CD24Fc treatment on immune population dynamics over time (**Fig 1E-F**). From baseline to D8, the CD24Fc group displayed a sharp and steady decline of plasma B cells (cluster 6), which coordinated with a proportional increase in mature B cells (cluster 8). The placebo group showed relatively stable cell proportions for these populations over the same time frame. There were no significant differences between the two groups in mounting an effective anti-Spike protein antibody response (**Fig S1**).

CD24Fc SUPPRESSES T CELL ACTIVATION. We developed a 25-marker flow cytometry panel to examine the intricacies associated with effector cell (NK and $CD4^+$/$CD8^+$ T cell) activation and differentiation in response to SARS-CoV-2 infection and CD24Fc treatment (**Table S2**). Using our unbiased clustering approach, we identified eight distinct clusters within $CD8^+$ T cells from COVID-19 and HD samples (**Fig 2A-C**). At baseline, COVID-19 samples showed enriched frequency of clusters 4, 5, 7, and 8, which express markers of activation; HD samples were skewed towards cluster 1, which exhibits a naive phenotype (**Fig. 2D-E**). To analyze the impact of CD24Fc on $CD8^+$ T cell activation, we generated UMAP contour plots for each treatment group (**Fig 2F**), and analyzed changes to cluster proportions over time (**Fig 2G**). CD24Fc treatment correlated with a modest increase in cluster 1 frequency over time, whereas placebo-treated patients showed marked decline. Conversely, the proportion of cluster 8 cells (a population whose expression pattern is suggestive of highly activated $CD8^+$ T cells) were stagnant in CD24Fc-treated patients, compared to the marked increase seen in placebo group (**Fig 2G**).

While tracking cluster proportions over time provides an unbiased global view of the data, these statistically-distinct cell clusters may not always correspond perfectly to biologically-distinct cell types. Therefore, we augmented the unbiased clustering analysis with a semi-supervised approach to define an unbiased $CD8^+$ T cell activation score. Known markers of T cell activation (T-bet, Ki-67, CD69, TOX, and GZMB) were significantly increased in baseline COVID-19 patients compared to HD (**Fig 2H**), supporting our hypothesis that SARS-CoV-2 infection increases peripheral T cell activation. To create a unified cell-

level activation score, we used PCA to implement dimension reduction of the cell-by-activation marker expression data for all baseline COVID-19 and HD cells. The first principal component (PC1) loadings of each activation marker were used as coefficients in a linear model for defining the activation score (**Table S3**). Thus, while we manually selected key T cell activation markers, we determined the relative contribution of each activation marker to the final activation score in an unbiased and data-adaptive manner, yielding a semi-supervised approach. We observed positive PC1 loadings and positive average log-fold changes for each activation marker, confirming that higher activation scores reflect higher T cell activation (**Table S3**). Distributions of activation scores across cell clusters also confirmed that more highly activated cell subsets feature higher activation scores (**Fig 2I**).

To characterize the effect of CD24Fc treatment on global $CD8^+$ T cell activation, we adopted a GLMM of the activation scores over time. While $CD8^+$ T cell activation scores at baseline were not statistically different between groups, the predicted mean activation scores indicate significantly different trajectories between placebo and CD24Fc groups over time (**Fig 2J**). Thus, we conclude that CD24Fc treatment significantly reduced $CD8^+$ T cell activation compared to placebo. $CD4^+$ T cell activation also plays an important role in immune response to SARS-CoV-2 infection, so we applied the analysis strategy presented above to this population[26]. To comprehensively understand the role of $CD4^+$ T cells and $FOXP3^+$ Tregs, we analyzed total $CD4^+$ T cells including $FOXP3^+$ subset (**Fig S2**), and then $FOXP3^+$ Tregs exclusively (**Fig S3**). Both analyses showed hyperactivated subsets and overall activation score decreased by CD24Fc treatment.

CD24Fc REDUCES NK CELL ACTIVATION. The increased number of NK cells in samples from patients with COVID-19 (**Fig 1C-D**, cluster 10) implies they play an important role in SARS-CoV-2 infection. We investigated the activation status of NK cells using our unbiased clustering and visualization approach, and identified 12 statistically-distinct NK cell clusters, which we visualized on heatmaps and UMAPs (**Fig 3A-C**). Cluster 5, the most highly represented cluster in HD samples, displayed an expression pattern suggestive of a less activated population. Samples from COVID-19 patients revealed significant reduction in cluster 5 and expansion of clusters 4, 6, 8, 9, 10, 11, and 12 (**Fig 3D-E**).

To understand the role of CD24Fc treatment on NK cell population dynamics, we generated UMAP contour plots to visualize temporal and treatment-based changes (**Fig 3F**), and quantified these differences (**Fig 3G**). Clusters 1 and 2, which show mild activation, were increased by CD24Fc, while cluster 11, which expresses multiple activation markers, was decreased. To visualize activation, known NK cell activation markers (TOX, GZMB, KLRG1, Ki-67, and LAG3) were assessed (**Fig 3H**) and plotted per cluster (**Fig 3I**). Using a GLMM of activation scores over time, we found that while baseline values for NK cell activation were not statistically different, the mean activation scores were significantly different between placebo and CD24Fc groups throughout the study duration (**Fig 3J**). Thus, CD24Fc treatment rapidly reduced NK cell activation status, and the impact was sustained throughout the study period.

CD24Fc ATTENUATES SYSTEMIC CYTOKINE RESPONSE. To examine the effect of CD24Fc on cytokine response to SARS-CoV-2 infection, we compared plasma cytokine concentrations from HD and COVID-19 patients treated with CD24Fc or placebo. We used multiplex ELISA and Luminex analysis platforms testing 37 cytokines in total. Fifteen out of 37 tested cytokines were significantly elevated during SARS-CoV-2 infection (**Fig 4A**, **Fig S4A**). These included cytokines associated with type 1 (IL-12p40, CXCL9, IL-15) and type 3 (IL-1α, IL-1β, RANTES) immunity, and chemokine MCP-1 (CCL2) that recruits monocytes and T cells to the sites of inflammation. Only three out of 37 cytokines were significantly downregulated in COVID-19 patients (**Fig S4A**).

We next studied the impact of CD24Fc on cytokine expression in patients with COVID-19. As shown in **Fig 4B**, substantial reduction of cytokines (GM-CSF, IL-5, IL-7, IL-10) and chemokines (MIG, MIP-1α, MIP-1β) was observed within 24 hours of CD24Fc. At 1 week after treatment, most of the cytokines and chemokines tested are reduced by 10-fold or more. The majority of them are selectively reduced in the CD24Fc-treated patients including cytokines critically involved in COVID-19 pathogenesis, such as IL-6 and GM-CSF[30]. Analysis of cytokine scores calculated by integrating expression of all markers tested by multiplex ELISA platform using weighted sum approach demonstrated significant decrease in CD24Fc-treated groups compare to placebo (**Fig 4C**). This finding was independently confirmed using Autoencoder[20] and PCA (**Fig S4D**).

To better understand this modulation, we studied correlations between individual cytokines across groups. Correlation matrices (**Fig 4F**) showed that only a few groups of cytokines were co-expressed by HD. The numbers of co-regulated cytokines dramatically increased in baseline COVID-19 samples indicating activation of coordinated cytokine response. Remarkably, samples from CD24Fc-treated patients (pooled over time) showed a decline in cytokine correlations compared to baseline or placebo treatment. Similarly, cytokine network plots connecting cytokines with moderate and strong associations (Pearson correlation $r>0{\cdot}4$[21]) showed lower overall interconnectedness in CD24Fc group as compared to baseline or placebo treatment (**Fig 4G**). The overall cytokine network correlations and connectivity in CD24Fc-treated patients were significantly different from baseline or placebo treatment (**Fig 4H-I**).

To understand the relevance of decreased correlation and connectivity of the cytokine network in CD24Fc-treated patients to disease severity and therapeutic effect, we performed a similar analysis using a previously published dataset of cytokine expression in serum from patients with COVID-19 who were either treated in the intensive care unit (ICU patients) or did not require ICU treatment (non-ICU patients)[31]. Notably, we found that inter-cytokine correlation and connectivity was lower in non-ICU patients than ICU patients (**Fig S5**). These data suggest that increased blood cytokine network correlation and connectivity are associated with increased COVID-19 disease severity, while mild disease (without the need for ICU treatment) is characterized by lower correlation and connectivity. Therefore, decreased correlation and connectivity of the cytokine network in CD24Fc-treated patients are likely evidence of therapeutic efficacy.

To identify factors that may play an important role in response to CD24Fc, we calculated centrality scores[24] for individual cytokines based on their connectivity and correlations within the global cytokine network (**Table S4** and **S5**). The variances of the centrality scores of 30 cytokines were lower in baseline and placebo-treated COVID-19 patients compared to HD and CD24Fc-treated COVID-19 patients (**Fig 4J**). These data indicate that distinct cytokines are highly heterogeneous in terms of their interconnectedness with other cytokines (centrality) in healthy individuals. Upon SARS-CoV-2 infection, cytokine centralities become more uniform and subsequent CD24Fc treatment abrogates this effect (**Fig 4J**).

DISCUSSION

Patients enrolled in the SAC-COVID clinical trial, a subpopulation of which were studied herein, demonstrated accelerated clinical recovery following CD24Fc treatment compared to placebo. CD24Fc was generally well-tolerated, reduced disease progression, and shortened hospital length of stay (results under review in Welker J *et al.* "Therapeutic Efficacy and Safety of CD24Fc in Hospitalised Patients with COVID-19," submitted to *Lancet*). Given the proposed mechanism of action and pathophysiology of SARS-CoV-2, we hypothesized that CD24Fc reduced the hyperactive systemic immune responses in infected patients leading to accelerated return to homeostasis. Using deep immune profiling of longitudinal samples combined with our deep bioinformatic analysis, we uncovered the effects of CD24Fc on the systemic host immune response. Overall, we found that CD24Fc treatment blunted immune cell activation across several compartments and facilitated return to a more normal phenotype following SARS-CoV-2

infection.

Comparing baseline COVID-19 patients with HD allowed us to identify the immune cell populations driving pathogenesis. As expected, we saw a significant increase in activated $CD8^+$ T and NK cells in SARS-CoV-2-infected patients. We augmented the unbiased clustering analysis with a semi-supervised approach to define an unbiased activation score. CD24Fc-treated patients demonstrated significant reduction in activation score over time for both $CD8^+$ T and NK cells compared to placebo-treated patients.

The changes in population dynamics between HD and COVID-19 patients are intriguing and offer two separate interpretations. CD24Fc may preferentially block the differentiation of mature B cells into effector plasma cells, resulting in relatively fewer plasma B cells (cluster 6) and more mature B cells (cluster 8). Alternatively, CD24Fc treatment may reduce the systemic burden of SARS-CoV-2 infection, which would limit the number of plasma cells due to accelerated recovery. In either scenario, the correlation between decreased circulating plasma cells in CD24Fc-treated patient samples suggests significant immuno-modulatory roles in this treatment. The ability of patients to mount an effective anti-Spike antibody response was not compromised by CD24Fc treatment.

Aberrant and rapid increase in a broad spectrum of pro-inflammatory cytokines, known as a cytokine storm, plays a central role in pathogenesis of ARDS and other severe complications of SARS-CoV-2 infection[32]. Unlike the cytokine storm associated with immunotherapy, which can be effectively treated by antibodies targeting IL-6R, treating COVID-19 with the same antibodies has shown limited success. Our longitudinal analysis revealed a broad-spectrum up-regulation of systemic cytokines in patients with severe COVID-19. More importantly, CD24Fc treatment cause rapid and sustained reduction of most of the 30 cytokines/chemokines tested. Among them are known COVID-19 therapeutic targets such as IL-6 and GM-CSF. This broad effect may explain the significant therapeutic efficacy of CD24Fc in treating hospitalized COVID-19 patients.

In addition to the two therapeutic targets, we also identified two cytokines that were significantly downregulated after CD24Fc treatment: IL-10 and IL-15. Both are linked with COVID-19 severity, increased intensive care admission, and/or COVID-19-associated death[33-35]. Although generally associated with immunosuppressive functions, IL-10 can also stimulate NK and $CD8^+$ T cells and induce B cell proliferation and antibody production[36]. IL-15 promotes activation and expansion of NK and $CD8^+$ T cells[37,38]. Thus, CD24Fc may blunt NK and $CD8^+$ T cell activation by suppressing IL-10 and IL-15 production. Since IL-15 also promotes activation and recruitment of neutrophils to site of inflammation, CD24Fc may suppress COVID-19-associated neutrophil activation and/or neutrophilia[39]. Furthermore, CD24Fc may limit viral replication by suppressing IL-10 production, which has been shown to enhance viral replication of HIV, HCV and HBV[40].

Importantly, unlike HD, COVID-19 patients displayed strong positive correlations between inflammatory cytokines, consistent with broad misfiring of host immune responses[29,31,41]. Notably, CD24Fc treatment reduced systemic cytokine levels and diminished correlations and connectivity in SARS-CoV-2-infected individuals, thus reshaping the systemic cytokine network towards a less tightly co-regulated state characteristic of homeostasis. Based on analysis of the global cytokine landscape, we conclude that CD24Fc mitigates the exacerbated host systemic inflammatory responses to SARS-CoV-2. This conclusion was corroborated by the decrease of cytokine correlation and connectivity in patients with mild COVID-19 infections as compared to patients with severe disease that required an ICU treatment. A detailed investigation of individual inflammatory markers revealed potential mechanisms of COVID-19 severity reduction by CD24Fc.

In conclusion, the data presented here offer unique immunological insights that underscore the clinical

findings of the SAC-COVID trial. These results strongly support further investigation of CD24Fc for various inflammatory conditions including COVID-19. Our unique cytokine centrality analysis and cellular activation index also warrants further study as a prognostic tool for guiding therapy in COVID-19 and other systemic inflammatory conditions.

Acknowledgements and Funding. This work was supported in part by National Institutes of Health (NIH) grants, including R01AI077283, R01CA213290 to Z.L; and R37CA233770 to A.E.V. Z.L is also supposed by funding from the Pelotonia Foundation. Research reported in this publication was also supported by The Ohio State University Comprehensive Cancer Center and the NIH under grant number P30CA016058.

We acknowledge the patients who agreed to participate in this clinical trial, as the forward trajectory of science hinges on their support. We acknowledge Oncoimmune (now part of Merck & Co., Inc., Kenilworth, NJ, USA) for designing and supporting the clinical trial, which allowed us to collect samples for our correlative studies. The correlative studies were not part of the original phase III Oncoimmune trial, but were done at The Ohio State University trial site after communication of intent and sample collection. We thank the staff and researchers in the Pelotonia Institute for Immuno-Oncology for their support during the course of the study. We appreciate the expert administrate support by Ms. Teresa Kutcher.

REFERENCES

1. Hoffmann M, Kleine-Weber H, Schroeder S, et al. SARS-CoV-2 Cell Entry Depends on ACE2 and TMPRSS2 and Is Blocked by a Clinically Proven Protease Inhibitor. *Cell* 2020; **181**(2): 271-80 e8.
2. Cicco S, Cicco G, Racanelli V, Vacca A. Neutrophil Extracellular Traps (NETs) and Damage-Associated Molecular Patterns (DAMPs): Two Potential Targets for COVID-19 Treatment. *Mediators Inflamm* 2020; **2020**: 7527953.
3. Cao X. COVID-19: immunopathology and its implications for therapy. *Nat Rev Immunol* 2020; **20**(5): 269-70.
4. Thompson MG, Burgess JL, Naleway AL, et al. Prevention and Attenuation of Covid-19 with the BNT162b2 and mRNA-1273 Vaccines. *N Engl J Med* 2021; **385**(4): 320-9.
5. Planas D, Veyer D, Baidaliuk A, et al. Reduced sensitivity of SARS-CoV-2 variant Delta to antibody neutralization. *Nature* 2021; **596**(7871): 276-80.
6. Bergwerk M, Gonen T, Lustig Y, et al. Covid-19 Breakthrough Infections in Vaccinated Health Care Workers. *N Engl J Med* 2021.
7. Corey L, Beyrer C, Cohen MS, Michael NL, Bedford T, Rolland M. SARS-CoV-2 Variants in Patients with Immunosuppression. *N Engl J Med* 2021; **385**(6): 562-6.
8. Consortium WHOST, Pan H, Peto R, et al. Repurposed Antiviral Drugs for Covid-19 - Interim WHO Solidarity Trial Results. *N Engl J Med* 2021; **384**(6): 497-511.
9. Simonovich VA, Burgos Pratx LD, Scibona P, et al. A Randomized Trial of Convalescent Plasma in Covid-19 Severe Pneumonia. *N Engl J Med* 2021; **384**(7): 619-29.
10. Stone JH, Frigault MJ, Serling-Boyd NJ, et al. Efficacy of Tocilizumab in Patients Hospitalized with Covid-19. *N Engl J Med* 2020; **383**(24): 2333-44.
11. Group RC, Horby P, Lim WS, et al. Dexamethasone in Hospitalized Patients with Covid-19. *N Engl J Med* 2021; **384**(8): 693-704.
12. Tian RR, Zhang MX, Zhang LT, et al. CD24 and Fc fusion protein protects SIVmac239-infected Chinese rhesus macaque against progression to AIDS. *Antiviral Res* 2018; **157**: 9-17.
13. Liu Y, Zheng P. CD24: a genetic checkpoint in T cell homeostasis and autoimmune diseases. *Trends Immunol* 2007; **28**(7): 315-20.
14. Toubai T, Hou G, Mathewson N, et al. Siglec-G-CD24 axis controls the severity of graft-versus-host disease in mice. *Blood* 2014; **123**(22): 3512-23.
15. Park LM, Lannigan J, Jaimes MC. OMIP-069: Forty-Color Full Spectrum Flow Cytometry Panel for Deep Immunophenotyping of Major Cell Subsets in Human Peripheral Blood. *Cytometry A* 2020; **97**(10): 1044-51.
16. Zeng C, Evans JP, Pearson R, et al. Neutralizing antibody against SARS-CoV-2 spike in COVID-19 patients, health care workers, and convalescent plasma donors. *JCI Insight* 2020; **5**(22).
17. Lo K, Brinkman RR, Gottardo R. Automated gating of flow cytometry data via robust model-based clustering. *Cytometry A* 2008; **73**(4): 321-32.
18. Scott AC, Dundar F, Zumbo P, et al. TOX is a critical regulator of tumour-specific T cell differentiation. *Nature* 2019; **571**(7764): 270-4.
19. Kallies A, Good-Jacobson KL. Transcription Factor T-bet Orchestrates Lineage Development and Function in the Immune System. *Trends Immunol* 2017; **38**(4): 287-97.
20. Liou C-Y, Cheng W-C, Liou J-W, Liou D-R. Autoencoder for words. *Neurocomputing* 2014; **139**: 84-96.
21. Schober P, Boer C, Schwarte LA. Correlation Coefficients: Appropriate Use and Interpretation. *Anesth Analg* 2018; **126**(5): 1763-8.
22. Gao J, Tarcea VG, Karnovsky A, et al. Metscape: a Cytoscape plug-in for visualizing and interpreting metabolomic data in the context of human metabolic networks. *Bioinformatics* 2010; **26**(7): 971-3.
23. Shannon P, Markiel A, Ozier O, et al. Cytoscape: a software environment for integrated models of biomolecular interaction networks. *Genome Res* 2003; **13**(11): 2498-504.

24. Valente TW, Coronges K, Lakon C, Costenbader E. How Correlated Are Network Centrality Measures? *Connect (Tor)* 2008; **28**(1): 16-26.
25. Tang Y, Li M, Wang J, Pan Y, Wu FX. CytoNCA: a cytoscape plugin for centrality analysis and evaluation of protein interaction networks. *Biosystems* 2015; **127**: 67-72.
26. Chen Z, John Wherry E. T cell responses in patients with COVID-19. *Nat Rev Immunol* 2020; **20**(9): 529-36.
27. Laing AG, Lorenc A, Del Molino Del Barrio I, et al. A dynamic COVID-19 immune signature includes associations with poor prognosis. *Nat Med* 2020; **26**(10): 1623-35.
28. Weiskopf D, Schmitz KS, Raadsen MP, et al. Phenotype and kinetics of SARS-CoV-2-specific T cells in COVID-19 patients with acute respiratory distress syndrome. *Sci Immunol* 2020; **5**(48).
29. Mathew D, Giles JR, Baxter AE, et al. Deep immune profiling of COVID-19 patients reveals distinct immunotypes with therapeutic implications. *Science* 2020; **369**(6508).
30. Thwaites RS, Sanchez Sevilla Uruchurtu A, Siggins MK, et al. Inflammatory profiles across the spectrum of disease reveal a distinct role for GM-CSF in severe COVID-19. *Sci Immunol* 2021; **6**(57).
31. Lucas C, Wong P, Klein J, et al. Longitudinal analyses reveal immunological misfiring in severe COVID-19. *Nature* 2020; **584**(7821): 463-9.
32. Leisman DE, Ronner L, Pinotti R, et al. Cytokine elevation in severe and critical COVID-19: a rapid systematic review, meta-analysis, and comparison with other inflammatory syndromes. *Lancet Respir Med* 2020; **8**(12): 1233-44.
33. Angioni R, Sanchez-Rodriguez R, Munari F, et al. Age-severity matched cytokine profiling reveals specific signatures in Covid-19 patients. *Cell Death Dis* 2020; **11**(11): 957.
34. Abers MS, Delmonte OM, Ricotta EE, et al. An immune-based biomarker signature is associated with mortality in COVID-19 patients. *JCI Insight* 2021; **6**(1).
35. Han H, Ma Q, Li C, et al. Profiling serum cytokines in COVID-19 patients reveals IL-6 and IL-10 are disease severity predictors. *Emerg Microbes Infect* 2020; **9**(1): 1123-30.
36. Wilson EB, Brooks DG. The role of IL-10 in regulating immunity to persistent viral infections. *Curr Top Microbiol Immunol* 2011; **350**: 39-65.
37. Younes SA, Freeman ML, Mudd JC, et al. IL-15 promotes activation and expansion of CD8+ T cells in HIV-1 infection. *J Clin Invest* 2016; **126**(7): 2745-56.
38. Verbist KC, Klonowski KD. Functions of IL-15 in anti-viral immunity: multiplicity and variety. *Cytokine* 2012; **59**(3): 467-78.
39. Cassatella MA, McDonald PP. Interleukin-15 and its impact on neutrophil function. *Curr Opin Hematol* 2000; **7**(3): 174-7.
40. Brooks DG, Trifilo MJ, Edelmann KH, Teyton L, McGavern DB, Oldstone MB. Interleukin-10 determines viral clearance or persistence in vivo. *Nat Med* 2006; **12**(11): 1301-9.
41. Chevrier S, Zurbuchen Y, Cervia C, et al. A distinct innate immune signature marks progression from mild to severe COVID-19. *Cell Rep Med* 2021; **2**(1): 100166.

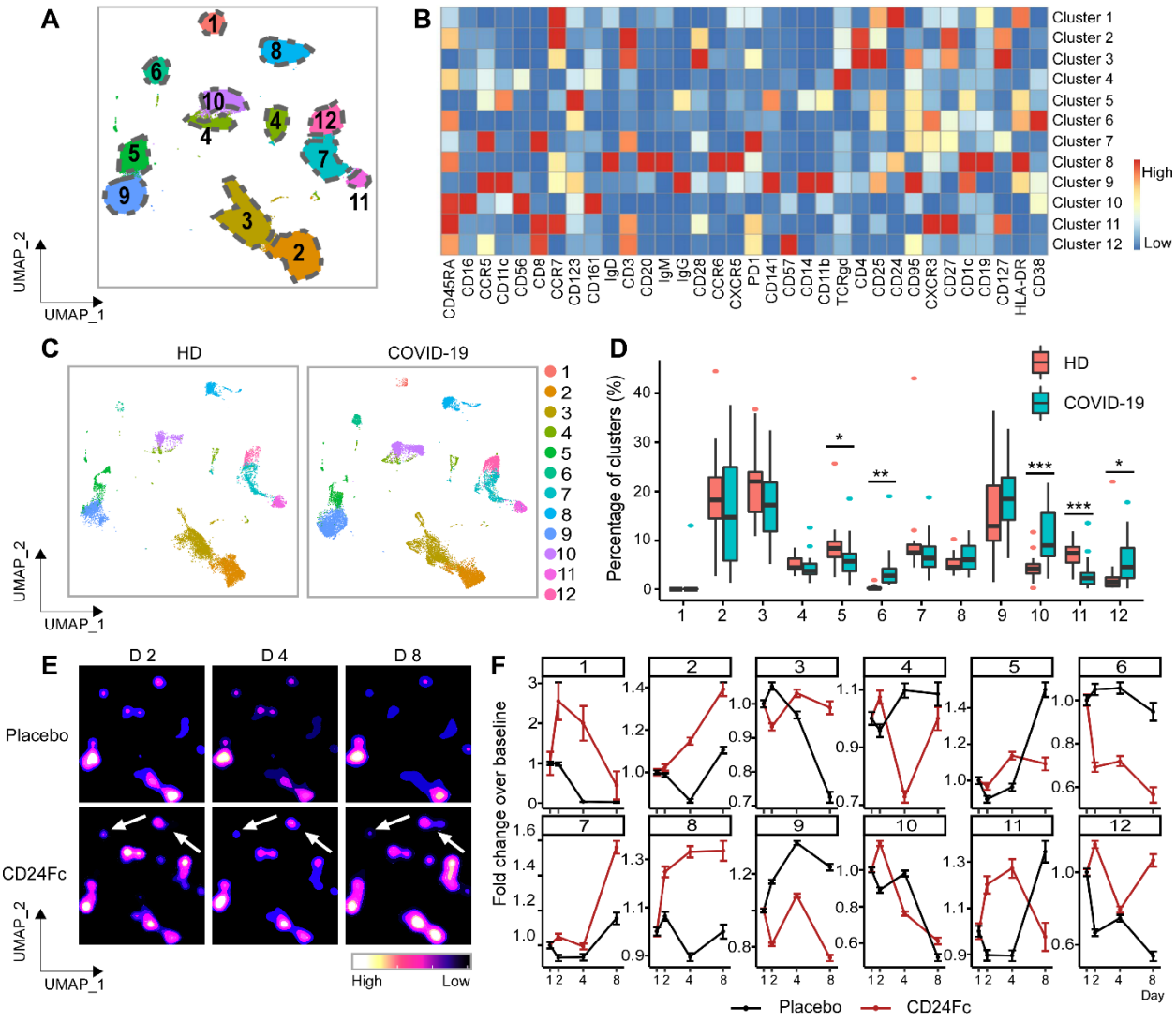

Figure 1. Population dynamics of peripheral blood mononuclear cells from healthy donors vs. patients with COVID-19 treated with placebo or CD24Fc.

A total of 1,306,473 PBMCs from HD (n=17) and COVID-19 patients (n=22) were clustered using an unbiased multivariate *t*-mixture model, which identified 12 sub-clusters that reflect statistically distinct cell states. Visualization of the relative similarity of each cell and cell cluster on the two-dimensional UMAP space with a 10% downsampling (**Panel A**). Cluster-by-marker heatmap characterizing the expression patterns of individual clusters (**Panel B**). UMAP dot plots (**Panel C**) and cluster frequencies (**Panel D**) of HD vs. baseline COVID-19 patient samples (cluster 5, p=0.03; cluster 6, p=0.001; cluster 10, p<0.001; cluster 11, p<0.001). Contour plots representing the density of cells throughout regions of the UMAP space from COVID-19 patients D2, D4, and D8 after CD24Fc vs. placebo treatment (**Panel E**, white arrows indicate visual changes between CD24Fc vs. placebo contour plots). Selected cluster population dynamics as fold change over baseline for each group over time (**Panel F**) (D2: placebo n=12, CD24Fc n=10; D4: placebo n=11, CD24Fc n=9; D8: placebo n=4, CD24Fc n=3). The p-value was calculated using the Kenward-Roger method. *, p<0.05; **, p<0.01; ***, p<0.001.

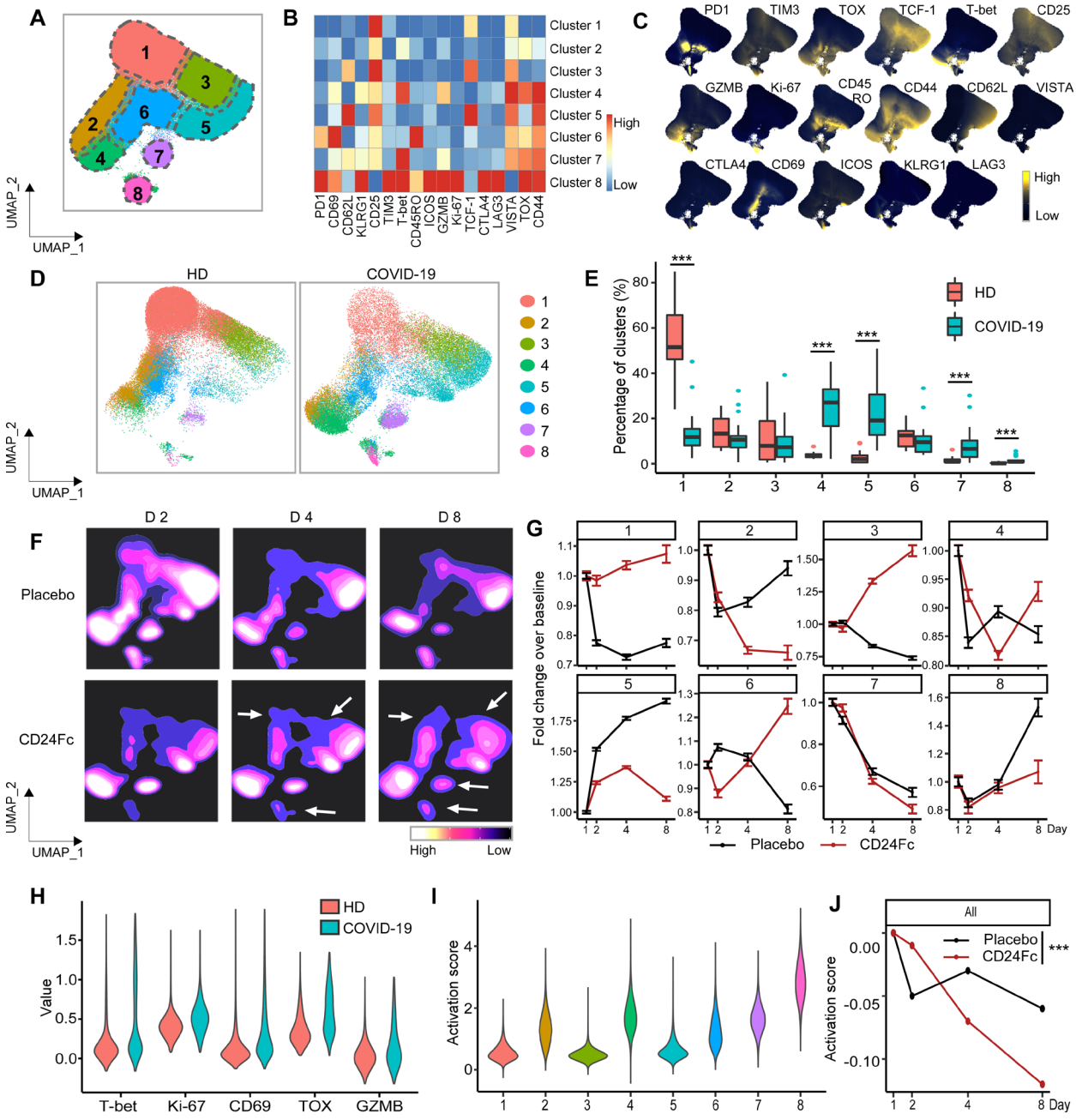

Figure 2. Subcluster analysis of peripheral blood CD8⁺ T cells in COVID-19 patients: activation following SARS-CoV2 infection is dampened by CD24Fc treatment.

A total of 1,466,822 CD8⁺ cells from HD (n=17) and COVID-19 (n=22) patients were clustered using an unbiased multivariate *t*-mixture model, which identified 8 CD8⁺ sub-clusters that reflect statistically distinct CD8⁺ T cell activation states. The relative similarity of each cell and cell cluster on the two-dimensional UMAP space were visualized with a 10% downsampling (**Panel A**). Using median expression of flow cytometry markers, a cluster-by-marker heatmap was generated to characterize the subsets (**Panel B**) and visualize individual marker expression patterns on the UMAP space (**Panel C**). To understand the effect of SARS-CoV2 infection on cell population dynamics, a comparison was made with UMAP dot plots (**Panel D**) and cluster frequencies (**Panel E**) of HD vs. baseline COVID-19 patient samples (cluster 1, $p<0.001$; cluster 4, $p<0.001$; cluster 5, $p<0.001$; cluster 7, $p<0.001$; cluster 8, $p<0.001$). The samples from COVID-

19 patients 2, 4, and 8 days after CD24Fc vs. placebo treatment were displayed using contour plots to represent the density of cells throughout regions of the UMAP space (**Panel F**, white arrows indicate visual changes between CD24Fc vs. placebo contour plots). The cluster population dynamics as fold change over baseline in each treatment group was shown (**Panel G**; sample distribution described in **Fig 1F** legend). To better characterize the activation status of CD8 T cells, a subset of markers (T-bet, Ki-67, CD69, TOX, GZMB) was linearly transformed to create a univariate cell-level activation score (**Panel H**), where highly activated cell clusters (such as cluster 8) had highest activation scores (**Panel I**). A GLMM was then to fit to the longitudinal cell-level activation scores to assess the effect of CD24Fc treatment on activation scores over time (**Panel J**). The p-value was calculated using the Kenward-Roger method. ***, $p<0.001$.

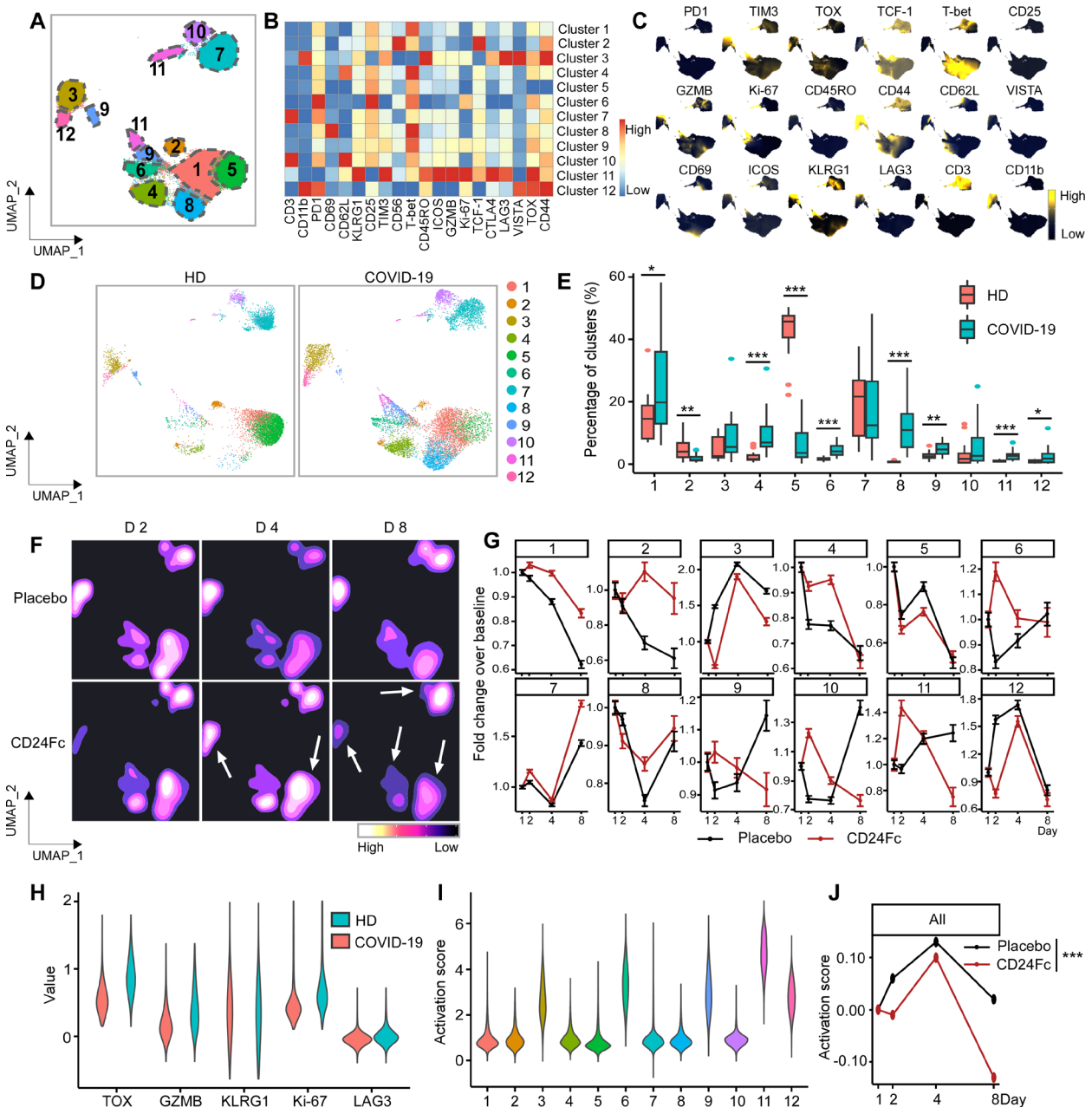

Figure 3. Subcluster analysis of peripheral blood NK cells in COVID-19 patients: activation of following SARS-CoV2 infection is dampened by CD24Fc treatment.

CD56$^+$ cells (n=783,623) from HD (n=17) and COVID-19 (n=22) patients were clustered using an unbiased multivariate *t*-mixture model, which identified 12 sub-clusters that reflect statistically distinct CD56$^+$ T cell activation states. The relative similarity of each cell and cell cluster on the two-dimensional UMAP space were visualized with a 10% downsampling (**Panel A**). Using median expression of flow cytometry markers, a cluster-by-marker heatmap were generated to characterize the subsets (**Panel B**) and visualize individual marker expression patterns on the UMAP space (**Panel C**). To understand the effect of SARS-CoV2 infection on NK cell population dynamics, a comparison was made with UMAP dot plots (**Panel D**) and cluster frequencies (**Panel E**) of HD vs. baseline COVID-19 patient samples. The day 2, 4, 8 samples from placebo and CD24Fc-treated patient groups were visualized using contour plots to represent the density of

cells throughout regions of the UMAP space (**Panel F**, white arrows indicate visual changes between CD24Fc vs. placebo contour plots). The cluster population dynamics as fold change over baseline in each treatment group was shown (**Panel G**; sample distribution described in **Fig 1** legend). To better characterize the activation status of NK cells, a subset of markers (TOX, GZMB, KLRG1, Ki-67, LAG-3) was linearly transformed to create a univariate cell-level activation score (**Panel H**), where highly activated cell clusters (such as cluster 11) had highest activation scores (**Panel I**). A GLMM was then fit to the longitudinal cell-level activation scores to assess the effect of CD24Fc treatment on activation scores over time (**Panel J**). The p-value was calculated using the Kenward-Roger method. *, $p<0.05$; **, $p<0.01$; ***, $p<0.001$.

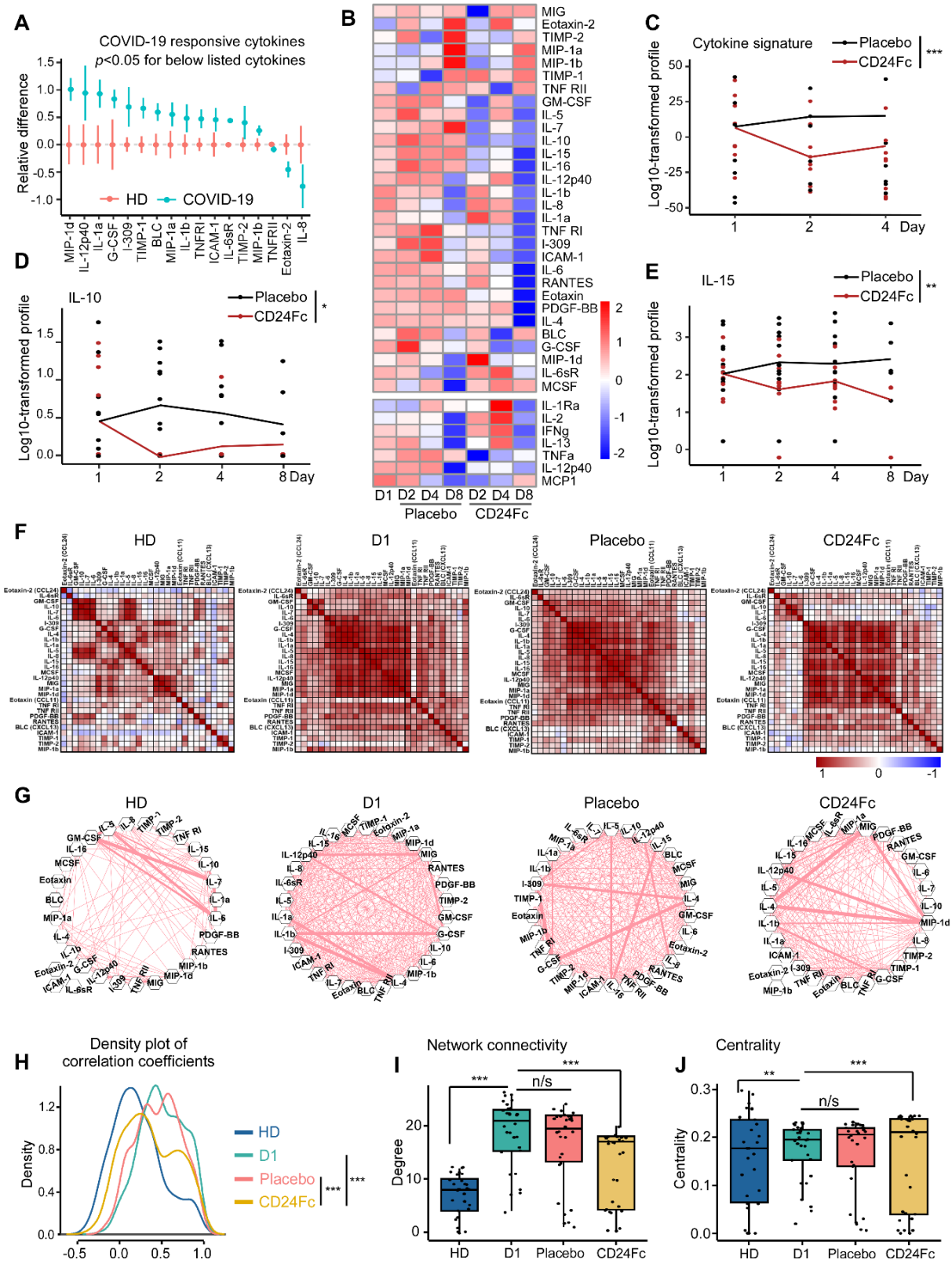

Figure 4. CD24Fc treatment downregulates systemic cytokine response in patients with COVID-19.

The relative differences in plasma concentrations of cytokines/chemokines between HD (n=25) and

COVID-19 patients (n=22) is shown. Values were log-transformed and evaluated using independent sample t-test. Only significantly up- and down-regulated markers are shown (**Panel A**). The heatmap analysis (**Panel B**) was used to visualize the relative levels of plasma cytokines/chemokines in placebo vs. CD24Fc-treated patients at indicated time points (Placebo: D1 n=12, D2 n=12, D4 n=11, D8 n=5; CD24Fc: D1 n=10, D2 n=10, D4 n=9, D8 n=3). To compare longitudinal patterns across groups, each cytokine had its group-specific baseline mean adjusted to match the overall mean at D1 and consequent time points are normalized accordingly, followed by scaling-by-row. The cytokine score was analyzed longitudinally using weighed sum approach (**Panel C**; $p<0.001$). Using log-10 transformation of cytokine concentrations (dots) and GLMM predicted fixed effects trends (lines), the changes in IL-10 (**Panel D**; $p=0.05$) and IL-15 (**Panel E**; $p=0.002$) levels in CD24Fc (red) and placebo (black) groups were revealed. Values and trend lines were centered at D1 mean. The p-value was calculated using the Kenward-Roger method. Using Pearson correlation matrices (**Panel F**; darker red indicates stronger correlation) and network maps (**Panel G**; weight of edge represents correlation coefficient), 30 plasma markers in HD (n=25), COVID-19 baseline (D1, n=22), placebo (pooled D2-D8, n=28), and CD24Fc-treated (pooled D2-D8, n=24) groups were visualized. Using these correlation coefficients, a density plot between 30 plasma cytokines (**Panel H**; D1 vs placebo, $p=0.07$; D1 vs CD24Fc, $p<0.001$; placebo vs CD24Fc, $p<0.001$) was constructed. Kolmogorov-Smirnov test was used to evaluate equality of densities between groups. Analysis of connectivity (**Panel I**) and centrality analysis of cytokine network (**Panel J**) display the cytokine expression relationships within each group. Network connectivity plots display highly correlated connections for each cytokine (i.e., node degree) and evaluated using paired t-test. Centrality analysis of cytokine network used eigenvector centrality score that considers global network connectivity and correlation coefficients between cytokines (HD vs D1, $p<0.001$; D1 vs placebo, $p=0.08$; D1 vs CD24Fc, $p<0.001$). Bartlett's test was performed to evaluate the significance of variance of centrality scores (HD vs D1, $p=0.013$; D1 vs placebo, $p=0.17$; D1 vs CD24Fc, $p=0.008$). Each dot in Panel I and J represents a cytokine. *, $p<0.05$; **, $p<0.01$; ***, $p<0.001$.

RESEARCH IN CONTEXT

Evidence before this study

We searched Pubmed, medRxiv, and bioRxiv from January 2020 for publications that studied the efficacy of therapeutic reagents and their effect on immune cell population dynamics and T and NK cells activation status in COVID-19 patients. Search terms used broadly were: immune cell dynamics in COVID-19 patients, effects of COVID-19 therapeutic reagents on immune system, COVID-19 immuno-pathology, CD24Fc and COVID-19. To our knowledge, extensive immune phenotyping and investigation of T and NK cell activation status has not been done in a phase III clinical trial setting evaluating therapeutic efficacy of CD24Fc. Existing approaches for characterizing T and NK cell activation have failed to succinctly model activation status as a function of treatment group over the course of the disease, thus preventing robust conclusions regarding the effect of treatment on immune cell dynamics in COVID-19 patients.

Added value of this study

In the SAC-COVID phase III clinical trial (NCT04317040), CD24Fc treatment accelerates recovery of patients with severe COVID-19 (clinical results under review in Welker J *et al*. "Therapeutic Efficacy and Safety of CD24Fc in Hospitalised Patients with COVID-19," submitted to *Lancet*). CD24Fc reduced disease progression and shortened hospitalization, with no apparent side effects. In the current manuscript, we show that CD24Fc reduces abnormal systemic inflammation as a key mechanism of action. We developed a statistical framework for characterizing T and NK cell activation longitudinally using repeated flow cytometry samples taken at each study timepoint. Our method is generalized and may be applied to uncover disease dynamics in other studies, especially in the context of COVID-19. Even though vaccines significantly reduce morbidity and mortality associated with SARS-CoV-2 infection, dexamethasone is the only therapeutic modality currently known to effectively treat patients with severe COVID-19. The emergence of variants such as the Delta variant, which shows evidence of escaping immunoprotection conferred by vaccination, emphasizes the importance of continued investigation into drugs that will mitigate severe COVID-19 symptoms. Development of drugs targeting the excessive immune response characteristic of COVID-19 remains crucial, and the data presented here and by Welker at al. support the use of CD24Fc to reduce morbidity and mortality associated with severe COVID-19.

Implications of all the available evidence

An excessive immune system activation upon SARS-CoV-2 infection can cause lethal complications and diseases progression mainly caused by cytokine storm. To counter this extreme immune responses, dexamethasone, well established anti-inflammatory reagent, has been used in clinic and showed its effectiveness in severe COVID-19 cases. CD24Fc, also showed therapeutic efficacy (Welker at al.) and here we studied potential mechanism of CD24Fc treatment. CD24Fc treatment systemically reduced activation of T and NK cells, and also reduced cytokines responsible for COVID-19 immunopathology. This suggests that CD24Fc can be used as a new therapeutic tool to treat COVID-19 patients.

SUPPLEMENTAL MATERIAL

This appendix has been provided by the authors to give readers additional information about their work.

TABLE OF CONTENTS

LIST OF INVESTIGATORS

Clinical Trial Site: The Ohio State University Wexner Medical Center 410 W. Tenth Ave, Columbus OH 43210

Clinical Laboratory Facility: OSUCCC Pelotonia Institute for Immuno-Oncology, 460 W. 12th Ave Room 580 Biomedical Research Tower, Columbus OH 43210

Clinical Investigators: Carlos Diego Malvestutto, M.D. M.P.H; Zeinab El Boghdadly, M.D.; Mohammad Mahdee Sobhanie, M.D.; Jose Bazan, D.O.; Mark Lustberg, M.D. Ph.D.; Susan Koletar, M.D.; Zihai Li, M.D. Ph.D.; Kelsi Reynolds; Karthik Chakravathy

Complete list of contributors (alphabetical): Carter Allen[1,3,4], Jose Bazan[2], Chelsea Bolyard[3], Zeinab El Boghdadly[2], Donna Bucci[3], Karthik B. Chakravarthy[3,11], Yuzhou Chang[1,3,4], Dongjun Chung[3,4], Martin Devenport[13], John P. Evans[12], Manuja Gunasena[8,9], Aastha Khatiwada[5], Susan Koletar[2], Amrendra Kumar[6,10], Anqi Li[1,3,11], Zihai Li[2,3], Shan-Lu Liu[12], Yang Liu[13], Namal P. M. Liyanage[8,9], Mark Lustberg[2], Anjun Ma[4], Qin Ma[4], Carlos D. Malvestutto[2], Kelsi Reynolds[3], Brian P. Riesenberg[3], Mohammad Mahdee Sobhanie[2], No-Joon Song[3], Zequn Sun[5], Maria Velegraki[3], Anna E. Vilgelm[3,6,10], Kevin P. Weller[3], Menglin Xu[2], Mohamed Yusuf[6], Cong Zeng[12], Pan Zheng[13].

Affiliations:
[1]The Ohio State University, Columbus, OH 43210, USA
[2]Department of Internal Medicine, The Ohio State University College of Medicine, Columbus, OH
[3]The Pelotonia Institute for Immuno-Oncology, The Ohio State University Comprehensive Cancer Center, Columbus, OH 43210, USA
[4]Department of Biomedical Informatics, The Ohio State University College of Medicine, Columbus, OH
[5]Department of Public Health Sciences, Medical University of South Carolina, Charleston, SC
[6]The Ohio State University Comprehensive Cancer Center, Columbus, OH 43210, USA
[7]Department of Microbiology, The Ohio State University College of Arts and Sciences, Columbus, OH 43210, USA
[8]Department of Microbial Infection and Immunity, The Ohio State University College of Medicine, Columbus, OH 43210, USA
[9]Department of Veterinary Biosciences, The Ohio State University College of Veterinary Medicine, Columbus, OH 43210, USA
[10]Department of Pathology, The Ohio State University College of Medicine, Columbus, OH
[11]The Ohio State University College of Medicine, Columbus, OH 43210, USA
[12]Center for Retrovirus Research and Department of Veterinary Biosciences, The Ohio State University, Columbus, OH 43210, USA
[13]OncoC4, Rockwille, MD, USA

Author contributions are as follows (alphabetically):
Study conception and design: D Bucci, M Devenport, Z Li, SL Liu, Y Liu, C Malvestutto, NJ Song, P Zeng
Acquisition of data: D Bucci, K Chakravarthy, JP Evans, M Gunasena, A Kumar, A Li, N Liyanage, C Malvestutto, K Reynolds, BP Riesenberg, NJ Song, M Velegraki, AE Vilgelm, K Weller, M Yusuf
Analysis and interpretation of data: C Allen, Y Chang, D Chung, JP Evans, K Chakravarthy, A Khatiwada, A Kumar, A Li, Z Li, SL Liu, N Liyanage, A Ma, Q Ma, BP Riesenberg, NJ Song, Z Sun, M Velegraki, AE Vilgelm, K Weller, M Xu, C Zeng
Drafting of manuscript: C Allen, C Bolyard, K Chakravarthy, D Chung, A Kumar, Z Li, SL Liu, N Liyanage, Q Ma, C Malvestutto, BP Riesenberg, NJ Song, AE Vilgelm, K Weller
Critical revision: C Allen, C Bolyard, D Chung, Z Li, SL Liu, BP Riesenberg, NJ Song
Other: Z Li, overall supervision of study activities; AE Vilgelm, acquisition of funding and supervision of cytokine studies; M Devenport, Y Liu, P Zheng for clinical study.

SUPPLEMENTARY METHODS

PATIENTS AND TRIAL PROCEDURE. This study included samples from patients enrolled in NCT04317040 at The Ohio State University Wexner Medical Center. Patients eligible for this trial were hospitalized with COVID-19, requiring supplemental oxygen but not mechanical ventilation, and had a prior positive SARS-CoV-2 PCR test. Enrolled patients were randomized in a double-blinded fashion by the hospital pharmacist to receive either a single dose of CD24Fc antibody (480mg IV infusion) or placebo control (IV saline). Peripheral blood samples were collected from patients prior to drug infusion (D1), and at subsequent time points 1, 3, 7, 14, and 28 days after drug infusion (D2, D4, D8, D15, and D29). Patients were monitored until D29, after which they completed the study endpoint. Pertinent patient clinical information was abstracted from the internal electronic medical record database including demographic data, medical history, clinical laboratory findings, and treatment regimen for COVID-19 during hospital stay (**Table S1**). All enrolled patients were able to complete the study endpoint with no demises in either group. After enrollment and completion of the study period, two patients were excluded from analysis. One exclusion was due to a diagnosis of chronic lymphocytic leukemia (CLL) which confounded the subsequent immunological analyses. Another exclusion occurred with a patient who received an infusion but was discharged before any post-infusion peripheral blood sample could be collected; hence no comparative analysis could be made using this patient. Written or witnessed oral informed consent was obtained for each patient. This trial and protocol were approved by Western Institutional Review Board. The study was monitored continuously by a clinical monitor and a medical monitor from the contract research organization (CRO) who also generated safety reports submitted to an independent Data and Safety Monitoring Board (DSMB). Data quality control checks were performed and medical monitor verified that the clinical trial was conducted and data was generated in compliance with protocol, International Conference on Harmonization Good Clinical Practice (ICH GCP) and all applicable regulatory requirements.

Patient characteristics were clinically matched between the two groups. All patients enrolled in the study received a treatment regimen for COVID-19 by hospital care teams regardless of their placebo/CD24Fc treatment status. Patients were randomized in a double-blind fashion into CD24Fc antibody treatment group (n=10) or placebo control group (n=12).

PBMC COLLECTION AND FLOW CYTOMETRY STAINING. Samples for this study were collected from patients enrolled in clinical trial NCT04317040. We analyzed samples from 22 patients hospitalized at The Ohio State University Wexner Medical Center with severe COVID-19. Peripheral blood mononuclear cells (PBMCs) were isolated per manufacturer's protocol using CPT tubes (BD Bioscience). Healthy donor (HD) PMBCs were obtained from STEMCELL Technologies™. We utilized a 36-color flow cytometry panel (**Table S2**, developed by Cytek[1]) to distinguish immune populations; we developed a 25-color panel (**Table S2**) to study activation status of $CD8^+$, $CD4^+$, and $CD56^+$ subsets. For the 25-color panel, surface markers were stained in 4°C for 1h and FOXP3/Transcription Factor Staining Buffer Set (eBioscience™) was used per manufacturers recommendation to perform intracellular staining. Cells were analyzed using the Cytek Aurora system.

VIRUS NEUTRALIZATION ASSAY. Virus was produced as previously described[2], and incubated with COVID-19 patient sera for 1h at 37°C. Virus was then overlaid onto ACE2-expressing 293T cells for 6h. Gluc activity was measured 24, 48, and 72 hours after infection.

CYTOKINE AND CHEMOKINE ASSAY. Plasma samples were processed using multiplexed ELISA-based platform Quantibody® Human Inflammation Array 3 (RayBiotech QAH-INF-3) in accordance with manufacturer's protocol. Slides were shipped to manufacturer site for scanning and data extraction services. Raw optical data were analyzed using manufacturer's analysis tool to construct standard curves and determine absolute cytokine concentrations. Cytokines for which standards did not yield good standard curve fit or that were undetectable were excluded (IFNγ, IL1rα, IL2, IL13, MCP-1, TNFα, TNFβ, IL-11, IL-12p70, IL-17A). Seven of these cytokines were detected using an alternative method. Specifically, cytokines IFNγ, IL1rα, IL2, IL13, MCP-1, TNFα, and IL-12p70 were measured by Luminex analysis. For that, plasma samples were sent to EVE Technologies that performed the assay and provided cytokine concentration data (**Table S6**).

FLOW CYTOMETRY DATA ANALYSIS. We integrated flow cytometry marker data from all samples and arcsinh scaling was applied using OMIQ (https://www.omiq.ai/). Then, we visualized cells in a reduced two-dimensional space using the UMAP algorithm implemented in the R package uwot[3]. We adopted a multivariate t-mixture model to cluster cells based on the normalized multivariate flow cytometry marker expression[4]. For each data set, we chose

the optimal number of cell clusters by selecting the model with the minimum Bayesian information criterion (BIC) score[5]. Then, we annotated cell types by visually investigating heatmaps of median marker expressions across clusters and expressions of these markers on the UMAP space.

IMMUNE CELL ACTIVATION SCORE CONSTRUCTION. To measure activation, we defined a cell-level immune cell activation score for each flow cytometry data set. We selected a subset of immune cell activation markers from the panel[6,7], and ran a principal component analysis (PCA) comparing cells from HD and baseline (Day 1) COVID patients, using these activation markers as features. We used the first principal component (PC1) as an activation score to reflect the differences in immune cell activation between groups. The loadings of each pre-selected activation marker onto PC1 were used as coefficients to compute an activation score for COVID-19 patients after baseline.

CYTOKINE SCORE CONSTRUCTION. To construct the cytokine score, we implemented a weighted sum approach, motivated by the polygenic risk score calculation in the genome-wide association study (GWAS). First, we fit a generalized linear mixed model (GLMM) of each cytokine measurement (base 10 log-transformed) on treatment, time, treatment*time, age, sex, and race as fixed-effect terms, along with subject-level random effect terms. Second, the *p*-value for evaluating the overall difference in trends between CD24Fc and placebo groups across all the time points was calculated using the Kenward-Roger method[8]. Finally, we obtained the weighted sum of cytokine measurements using the -2 log transformed *p*-value for the trend difference as weights, motivated by the Fisher's method. We validated the above approach using the PCA and autoencoder approaches[9].

NETWORK-LEVEL ANALYSIS OF CYTOKINE DATA. We first calculated Pearson correlation coefficients between cytokines (base 10 log-transformed). Then, we constructed a network, where a node represents a cytokine and an edge between two nodes was built if the corresponding absolute correlation coefficient is larger than 0.4, a cutoff that is usually considered to be moderate correlation[10]. The weight of an edge represents the corresponding correlation coefficient. A network was built via the MetScape[11] (version 3·1·3) application in Cytoscape[12] (version 3·8·0). We evaluated the network structure and the importance of each node in the network based on an eigenvector centrality (EC) score[13] using the CytoNCA[14] (version 2·1·6) application in Cytoscape (version 3.8.0). Nodes with larger EC scores can be considered of higher importance.

STATISTICAL ANALYSIS. All data were analyzed using the R statistical package. Group comparisons were evaluated using independent sample t-test or Kruskal-Wallis test for continuous variables, and Chi-squared test for categorical variables. In the longitudinal analyses, the overall differences in trends between CD24Fc and placebo groups across all the time points were evaluated using a GLMM of each measurement on treatment, time, treatment*time, age, sex, and race as fixed-effect terms, along with patient-level random intercepts. All mixed models were fit using the lme4 package[15]. The p-value for evaluating the overall difference in trends between CD24Fc and placebo groups across all the time points was calculated using the Kenward-Roger method[8]. The observed values and trend lines are centered at the baseline.

TREATMENT GROUP DETERMINATION. The treatment group (control vs. CD24Fc) was determined by the post-infusion sera to absorb anti-CD24 antibody for staining of human $CD24^+$ cells by flow cytometry. Patient group on the CD24Fc arm was further confirmed using CD24Fc ELISA (capture antibody: purified anti-human CD24, Clone ML5, BD bioscience, Cat#555426. San Jose, CA).

REFERENCES

1. Park LM, Lannigan J, Jaimes MC. OMIP-069: Forty-Color Full Spectrum Flow Cytometry Panel for Deep Immunophenotyping of Major Cell Subsets in Human Peripheral Blood. *Cytometry A* 2020; **97**(10): 1044-51.
2. Zeng C, Evans JP, Pearson R, et al. Neutralizing antibody against SARS-CoV-2 spike in COVID-19 patients, health care workers, and convalescent plasma donors. *JCI Insight* 2020; **5**(22).
3. McInnes L, Healy J, Melville J. UMAP: Uniform Manifold Approximation and Projection for Dimension Reduction. *arXiv preprint arXiv:180203426v3 [statML]* 2020.
4. Lo K, Brinkman RR, Gottardo R. Automated gating of flow cytometry data via robust model-based clustering. *Cytometry A* 2008; **73**(4): 321-32.
5. Schwarz G. Estimating the Dimension of a Model. *The Annals of Statistics* 1978; **6**(2): 461-4, 4.
6. Scott AC, Dundar F, Zumbo P, et al. TOX is a critical regulator of tumour-specific T cell differentiation. *Nature* 2019; **571**(7764): 270-4.
7. Kallies A, Good-Jacobson KL. Transcription Factor T-bet Orchestrates Lineage Development and Function in the Immune System. *Trends Immunol* 2017; **38**(4): 287-97.
8. Kenward MG, Roger JH. Small sample inference for fixed effects from restricted maximum likelihood. *Biometrics* 1997; **53**(3): 983-97.
9. Liou C-Y, Cheng W-C, Liou J-W, Liou D-R. Autoencoder for words. *Neurocomputing* 2014; **139**: 84-96.
10. Schober P, Boer C, Schwarte LA. Correlation Coefficients: Appropriate Use and Interpretation. *Anesth Analg* 2018; **126**(5): 1763-8.
11. Gao J, Tarcea VG, Karnovsky A, et al. Metscape: a Cytoscape plug-in for visualizing and interpreting metabolomic data in the context of human metabolic networks. *Bioinformatics* 2010; **26**(7): 971-3.
12. Shannon P, Markiel A, Ozier O, et al. Cytoscape: a software environment for integrated models of biomolecular interaction networks. *Genome Res* 2003; **13**(11): 2498-504.
13. Valente TW, Coronges K, Lakon C, Costenbader E. How Correlated Are Network Centrality Measures? *Connect (Tor)* 2008; **28**(1): 16-26.
14. Tang Y, Li M, Wang J, Pan Y, Wu FX. CytoNCA: a cytoscape plugin for centrality analysis and evaluation of protein interaction networks. *Biosystems* 2015; **127**: 67-72.
15. Bates D, Mächler M, Bolker B, Walker S. arXiv preprint. arXiv:14065823. 2014.
16. Lucas C, Wong P, Klein J, et al. Longitudinal analyses reveal immunological misfiring in severe COVID-19. *Nature* 2020; **584**(7821): 463-9.

SUPPLEMENTARY FIGURES

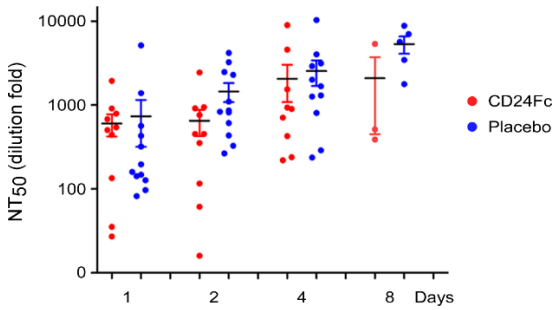

Figure S1. Comparison of neutralizing antibody against SARS-CoV-2 spike in CD24Fc treated patients and placebo group

Using our secreted nano luciferase-bearing pseudotyped lentivirus virus neutralization assay, we assessed the neutralizing antibody (nAb) titers for the CD24Fc treated and placebo groups throughout their treatment period. The average 50% neutralization titer (NT_{50}) for both groups show an increase in antibody titers from day 0 to day 15, but no significant differences were observed when CD24Fc group were compared to placebo group.

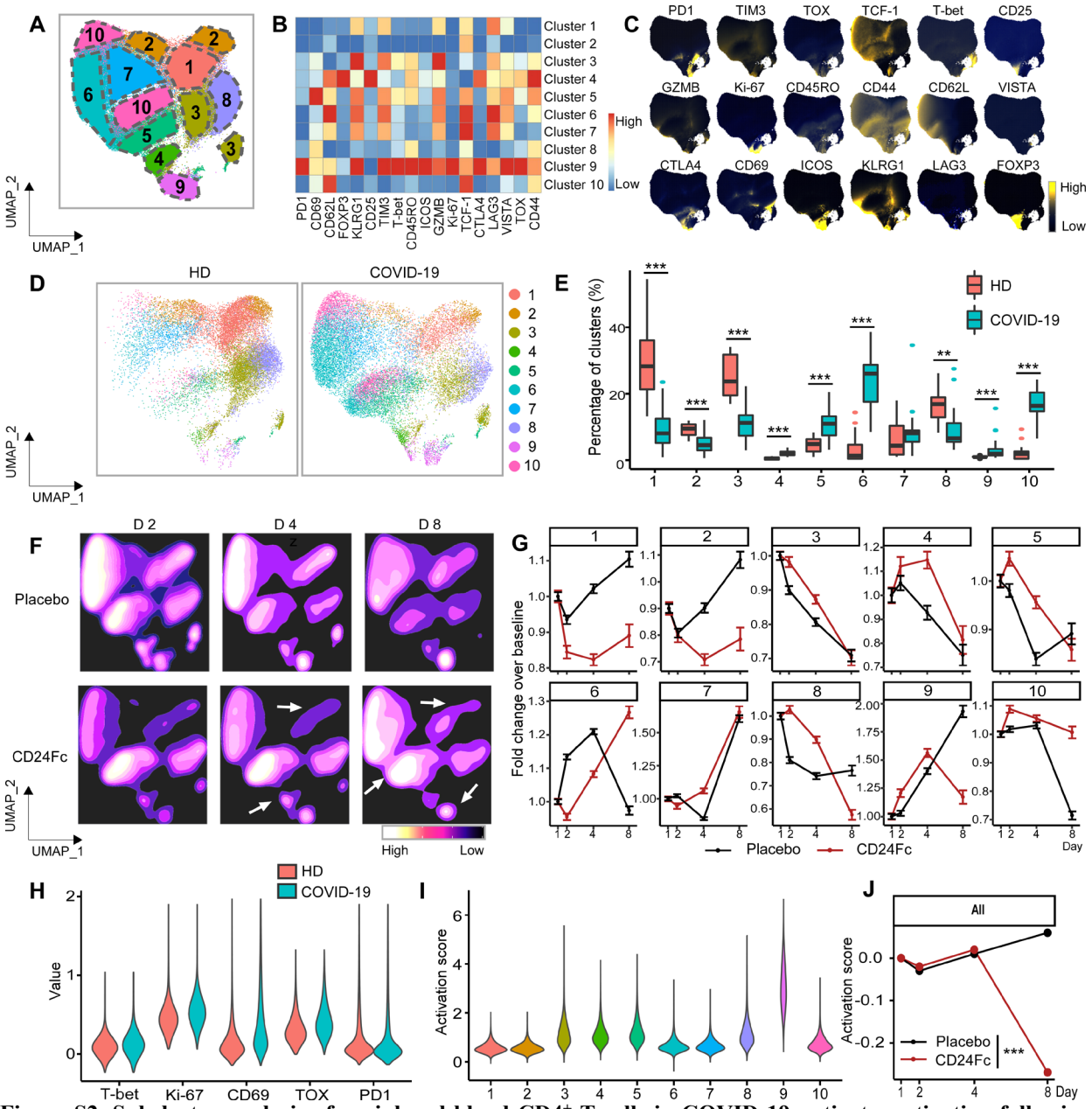

Figure S2. Subcluster analysis of peripheral blood CD4⁺ T cells in COVID-19 patients: activation following SARS-CoV2 infection is dampened by CD24Fc treatment.

We clustered 1,203,034 CD4⁺ cells from HD (n=17) and COVID-19 (n=22) patients using an unbiased multivariate *t*-mixture model, which identified 10 CD4⁺ sub-clusters that reflect statistically distinct cell activation states. We visualized the relative similarity of each cell and cell cluster on the two-dimensional UMAP space with a 10% downsampling (**Panel A**). Using median expression of flow cytometry markers, we generated a cluster-by-marker heatmap to characterize the subsets (**Panel B**) and visualized individual marker expression patterns on the UMAP space (**Panel C**). To understand the effect of SARS-CoV2 infection on cell population dynamics, we compared UMAP dot plots (**Panel D**) and cluster frequencies (**Panel E**) of HD vs. baseline COVID-19 patient samples (cluster 1, p<0·001; cluster 2, p<0·001; cluster 3, p<0·001; cluster 4, p<0·001; cluster 5, p<0·001; cluster 6, p<0·001; cluster 8, p=0·002; cluster 9, p<0·001; cluster 10, p<0·001). We visualized samples from COVID-19 patients D2, 4, and 8 after CD24Fc vs. placebo treatment using contour plots to represent the density of cells throughout regions of the UMAP space (**Panel F**). We describe cluster population dynamics as fold change over baseline in each treatment group (**Panel G**; sample distribution described in **Fig 1F** legend). To better characterize the activation status of CD4 T cells, we linearly transformed a subset of markers (T-bet, Ki-67, CD69, TOX, PD1) to create a univariate cell-level activation

score (**Panel H**), where highly activated cell clusters (such as cluster 9) had highest activation scores (**Panel I**). We then fit a GLMM to our longitudinal cell-level activation scores to assess the effect of CD24Fc treatment on activation scores over time (**Panel J**; p<0·001). The p-value for evaluating the overall difference in trends between CD24Fc and placebo groups across all time points was calculated using the Kenward-Roger method. Using this model, we found that CD24Fc-treated samples had significantly lower $CD4^+$ cell activation levels relative to placebo. **, p<0·01; ***, p<0·001.

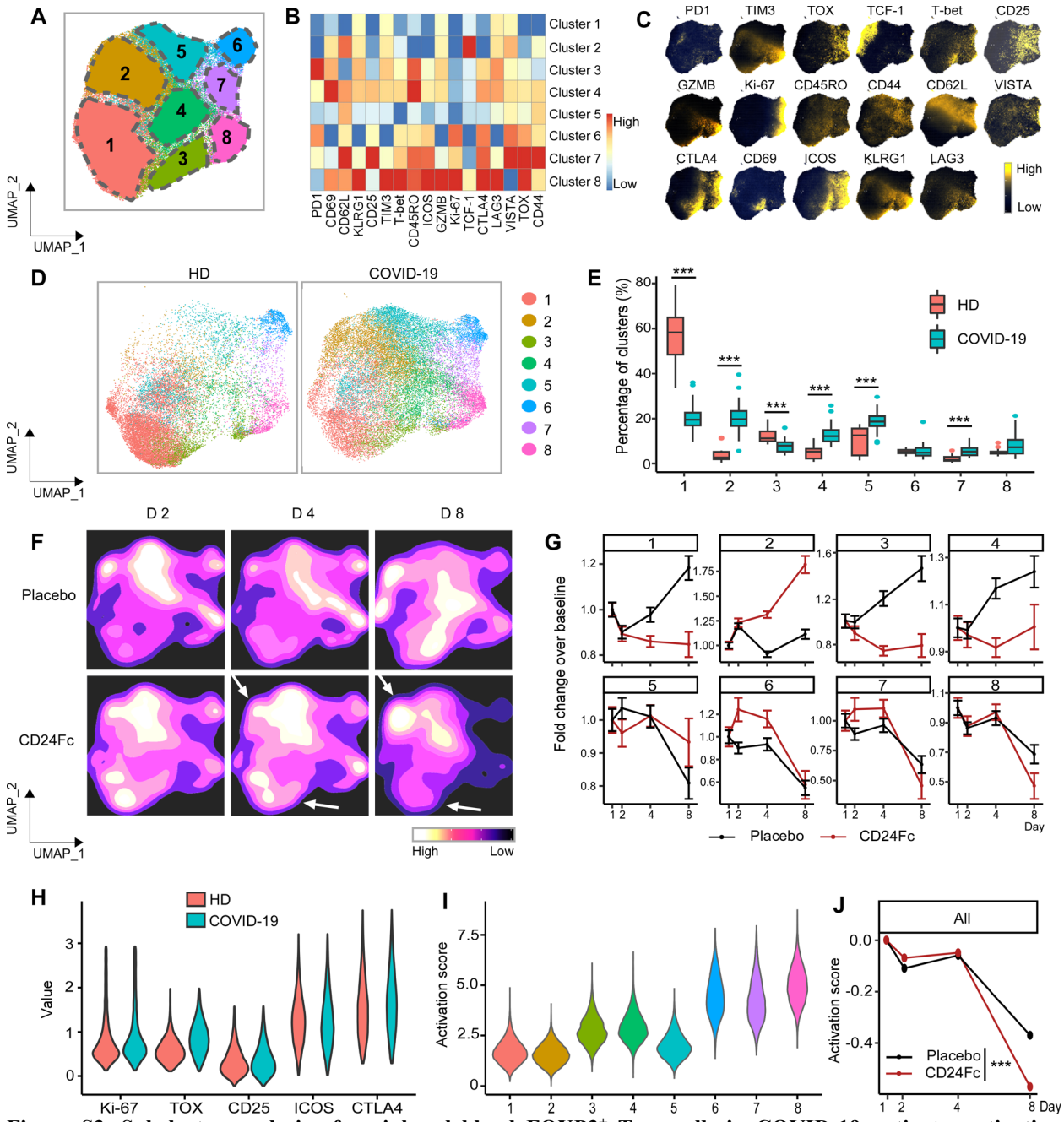

Figure S3. Subcluster analysis of peripheral blood FOXP3$^+$ Treg cells in COVID-19 patients: activation following SARS-CoV2 infection is dampened by CD24Fc treatment.

We clustered 98,525 FOXP3+ Treg cells from HD (n=17) and COVID-19 (n=22) patients using an unbiased multivariate *t*-mixture model, which identified 8 FOXP3$^+$ Treg sub-clusters that reflect statistically distinct cell activation states. We visualized the relative similarity of each cell and cell cluster on the two-dimensional UMAP space with a 10% downsampling (**Panel A**). Using median expression of flow cytometry markers, we generated a cluster-by-marker heatmap to characterize the subsets (**Panel B**) and visualized individual marker expression patterns on the UMAP space (**Panel C**). To understand the effect of SARS-CoV2 infection on cell population dynamics, we compared UMAP cluster frequencies of HD vs. baseline COVID-19 patient samples (**Panels D** and **E**). We visualized samples from COVID-19 patients D2, 4, and 8 after CD24Fc vs. placebo treatment using contour plots to represent the density of cells throughout regions of the UMAP space (**Panel F**). We describe cluster population dynamics as fold change over baseline in each treatment group (**Panel G**; sample distribution described in **Fig 1F** legend). To better characterize the activation status of Treg cells, we linearly transformed a subset of markers (Ki-67, TOX, CD25,

ICOS, CTLA4) to create a univariate cell-level activation score (**Panel H**), where highly activated cell clusters (such as clusters 6, 7 and 8) had highest activation scores (**Panel I**). We then fit a GLMM to our longitudinal cell-level activation scores to assess the effect of CD24Fc treatment on activation scores over time (**Panel J**). The p-value for evaluating the overall difference in trends between CD24Fc and placebo groups across all time points was calculated using the Kenward-Roger method. Using this model, we found that CD24Fc-treated samples had significantly lower Treg cell activation levels relative to placebo.

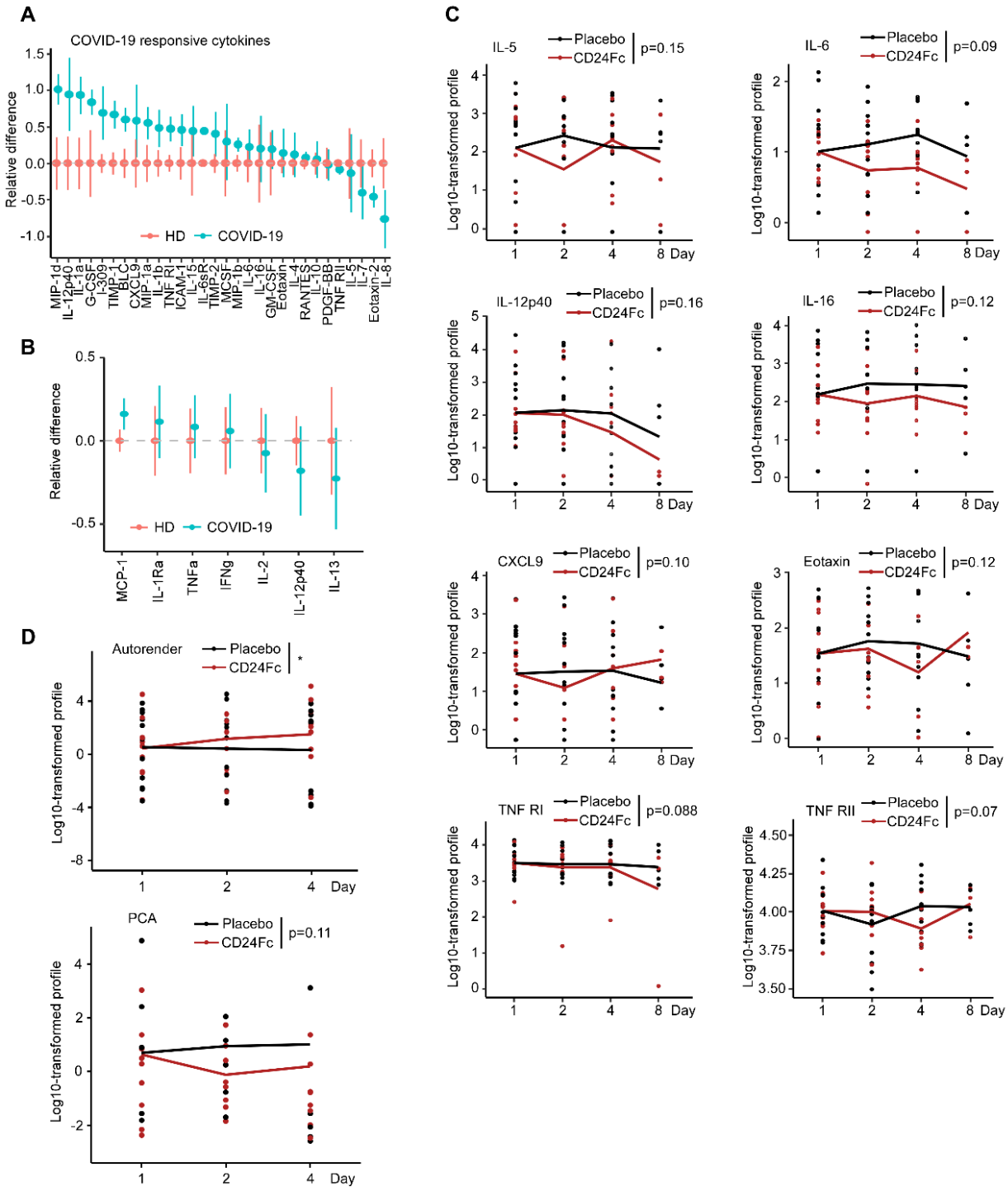

Figure S4. CD24Fc treatment downregulates systemic cytokines response in patients with COVID-19. We studied plasma cytokine and chemokine levels in HD and COVID-19 patients. Cytokine/chemokine measurements were log-transformed, and relative differences in cytokines in COVID-19 (n=22) compared to HD (n=25) samples were depicted (**Panel A and B**). Graph in Panel A shows data obtained using multiplex-ELISA platform, while graph in panel B presents data of cytokines measured by the Luminex analysis. Independent sample t-test was used to evaluate equality of average cytokine/chemokine levels. A number of other markers displayed trends towards decline in CD24Fc cohort compare to placebo, although these changes were not statistically significant (**Panel C**). Log-10 transformed cytokine measurement (dots) and GLMM predicted fixed effects trends (lines) of IL-5, IL-6, IL-12p40,

IL-16, CXCL9, Eotaxin, TNF R1 and TNF RII plasma concentrations in CD24Fc (red) and placebo (black) groups are displayed. The observed values and trend lines are centered at D1 mean. Longitudinal analysis of cytokine score was confirmed using both Autoencoder and PCA approaches (**Panel D**). We applied PCA and autoencoder on the base 10 log-transformed, centered and scaled cytokine data, and investigated the first two principal components (PCs) from the PCA and the three latent components from the autoencoder as cytokine scores. The autoencoder analysis was implemented using the Keras package. Specifically, we set one hidden layer for encoder and decoder, respectively, and three-dimensional embedding as latent layer output. All parameters were trained based on a 3-fold cross-validation. Due to missing data on D8, only D1, D2, and D4 data were used for the cytokine score calculation. For **Panels C** and **D**, the overall differences in trends between CD24Fc and placebo groups across all the time points were evaluated using a GLMM of each measurement. The p-value for evaluating the overall difference in trends between CD24Fc and placebo groups across all the time points was calculated using the Kenward-Roger method.

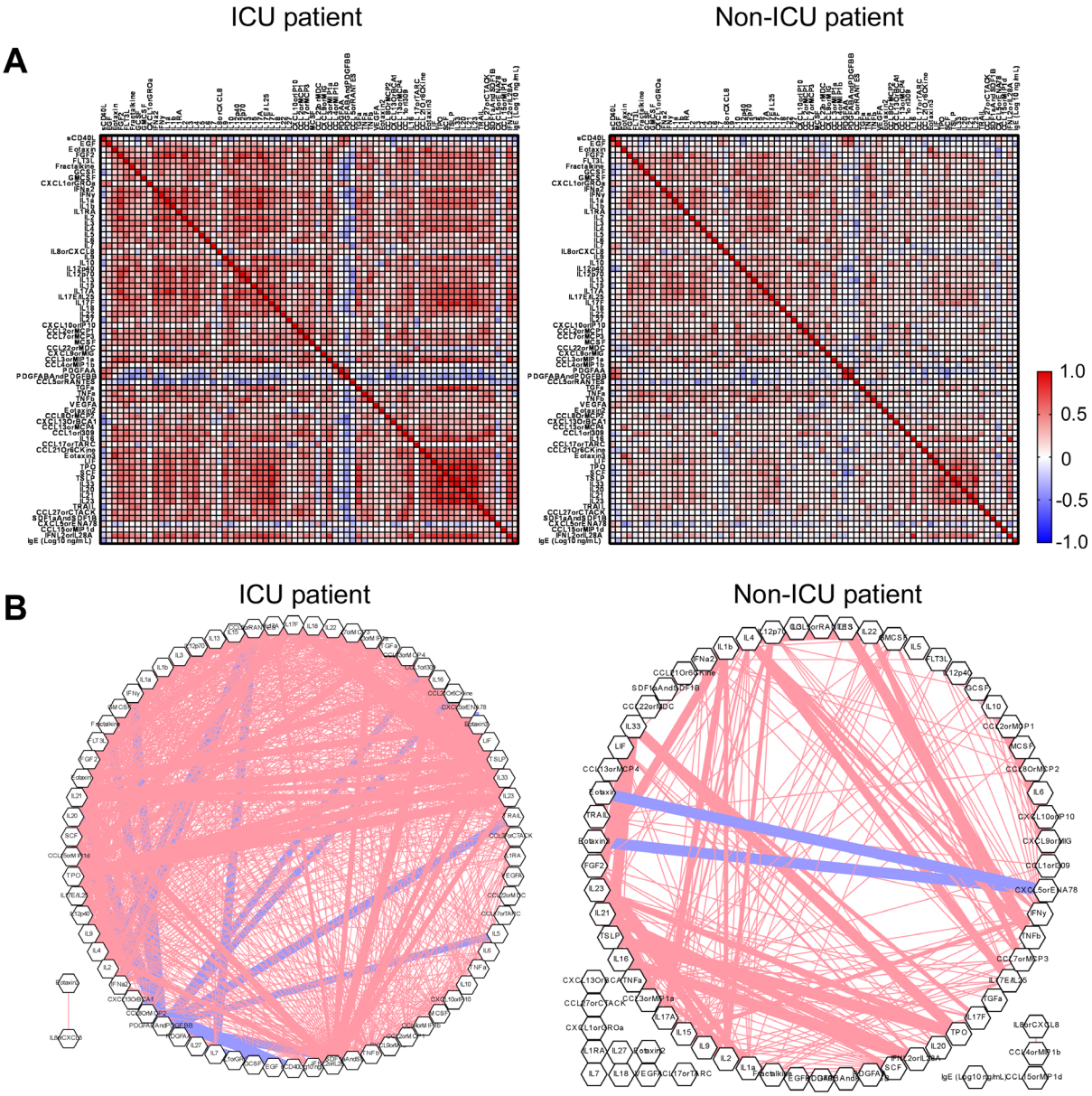

Figure S5. Patients with severe COVID-19 that require an ICU treatment display increased correlation and connectivity of the systemic cytokine network. We analyzed correlation (**Panel A**) and connectivity (**Panel B**) between circulating cytokines and chemokines in COVID-19 patients that either required (ICU patients), or did not require an ICU treatment (non-ICU patients). Cytokine measurements were obtained from previously published dataset [16]. Analysis was performed as described in **Fig 4**. A density plot constructed based on connectivity between plasma cytokines is shown in **Panel C**. **Panel D** shows an association between the severity of COVID-19 infection and the degree of the connectivity between plasma cytokines with severe UCU cases displaying higher degree of connectivity. The p-value was calculated using Wilcoxon Rank Sum test.

SUPPLEMENTARY TABLES

Table S1. Patient Characteristics.

CHARACTERISTIC **a) Demographics**	OVERALL (N=22)	PLACEBO (N=12)	CD24Fc (N=10)	P-value
BMI - median (IQR)	31.65 (28.18-38.83)	31.65 (29.41-39.52)	32.2 (28.1-37.88)	0.644
Age, yr - median (IQR)	57 (50.25-74.75)	60.5 (53.5-75)	55 (49.5-62)	0.62
<65 yr - no. (%)	15 (68.2)	7 (58.3)	8 (80.0)	
≥65 yr - no. (%)	7 (31.8)	5 (41.7)	2 (20.0)	
Sex - no. (%)				0.903
Female	8 (36.4)	5 (41.7)	3 (30.0)	
Male	14 (63.6)	7 (58.3)	7 (70.0)	
Race - no. (%)				0.528
White	16 (72.7)	9 (75.0)	7 (70.0)	
Black/AA	5 (22.7)	2 (16.7)	3 (30.0)	
Not Specified	1 (4.5)	1 (8.3)	0 (0.0)	
Ethnicity - no. (%)				0.724
Hispanic	4 (18.2)	3 (25.0)	1 (10.0)	
Non-Hispanic	18 (81.8)	9 (75.0)	9 (90.0)	
Smoking Hx - no. (%)	7 (31.8)	3 (25.0)	4 (40.0)	0.77
b) Co-existing Conditions				
Comorbidities - no. (%)				
Obesity (BMI ≥30)	12 (54.5)	7 (58.3)	5 (50.0)	1
Hypertension	11 (50.0)	5 (41.7)	6 (60.0)	0.669
Hyperlipidemia	8 (36.4)	5 (41.7)	3 (30.0)	0.903
Heart Disease	7 (31.8)	2 (16.7)	5 (50.0)	0.226
Diabetes	7 (31.8)	3 (25.0)	4 (40.0)	0.77
Autoimmune Condition	3 (13.6)	3 (25.0)	0 (0.0)	0.281
Cancer	2 (9.1)	1 (8.3)	1 (10.0)	1
HIV	1 (4.5)	0 (0.0)	1 (10.0)	0.926
COPD/Asthma	2 (9.1)	1 (8.3)	1 (10.0)	1
c) Clinical Information				
Baseline diastolic blood pressure, mm Hg - median (IQR)	65.5 (61.5-74)	67.5 (62.5-72)	65.5 (61.75-73.25)	0.766
Baseline systolic blood pressure, mm Hg - median (IQR)	127 (121-139.75)	138.5 (117.5-144)	124 (121.75-129)	0.137
Normotensive (<130) - no. (%)	12 (54.5)	5 (41.7)	7 (70.0)	0.369
Hypertensive (≥130) - no. (%)	10 (45.5)	7 (58.3)	3 (30.0)	
Baseline O_2 saturation on room air, % - median (IQR)	0.88 (0.84-0.9)	0.86 (0.8-0.88)	0.88 (0.85-0.9)	0.185
Hypoxic (<90) - no. (%)	16 (72.7)	10 (83.3)	6 (60.0)	0.458
Non-hypoxic (≥90) - no. (%)	6 (27.3)	2 (16.7)	4 (40.0)	
Baseline respiratory rate, respirations/min - median (IQR)	20 (18-25.5)	22 (19.5-28.5)	19 (16.5-21.5)	0.053
Eupnic (≤20) - no. (%)	13 (59.1)	6 (50.0)	7 (70.0)	0.607
Tachypnic (>20) - no. (%)	9 (40.9)	6 (50.0)	3 (30.0)	
Baseline heart rate, beats/min - median (IQR)	82.5 (67-91.75)	82.5 (73-91.25)	77.5 (66.25-92.5)	0.817
Eucardic (≤100) - no. (%)	22 (100.0)	12 (100.0)	10 (100.0)	n/a
Tachycardic (>100) - no. (%)	0 (0.0)	0 (0.0)	0 (0.0)	
Baseline temperature, °C - median (IQR)	37 (36.8-37.38)	36.95 (36.77-37.12)	37.15 (36.82-37.55)	0.466
Febrile (>37.0) - no. (%)	9 (40.9)	4 (33.3)	5 (50.0)	0.722
Non-febrile (≤37.0) - no. (%)	13 (59.1)	8 (66.7)	5 (50.0)	
Baseline RBC Count, M/μL - median (IQR)	4.61 (4.36-4.94)	4.61 (4.26-4.94)	4.62 (4.44-4.94)	0.598
Low (<4.3) - no. (%)	4 (18.2)	3 (25.0)	1 (10.0)	0.541
Normal (4.3-5.5) - no. (%)	15 (68.2)	8 (66.7)	7 (70.0)	
Elevated (>5.5) - no. (%)	3 (13.6)	1 (8.3)	2 (20.0)	
Baseline WBC Count, K/μL - median (IQR)	5.75 (5.23-8.07)	6.79 (5.34-7.98)	5.62 (4.85-8.78)	0.429
Low (<4.5) - no. (%)	2 (9.1)	0 (0.0)	2 (20.0)	0.124
Normal (4.5-11.0) - no. (%)	19 (86.4)	12 (100.0)	7 (70.0)	
Elevated (>11.0) - no. (%)	1 (4.5)	0 (0.0)	1 (10.0)	
Baseline Neutrophils, K/μL - median (IQR)	4.43 (3.9-6.8)	4.93 (4.3-6.38)	4.03 (3.15-6.75)	0.323
Baseline Lymphocytes, K/μL - median (IQR)	1.04 (0.76-1.33)	1.14 (0.69-1.6)	0.92 (0.85-1.21)	0.921
Baseline Monocytes, K/μL - median (IQR)	0.36 (0.29-0.57)	0.32 (0.25-0.5)	0.38 (0.34-0.57)	0.235
Baseline Eosinophils, K/μL - median (IQR)	0.04 (0.04-0.06)	0.04 (0.04-0.04)	0.04 (0.04-0.06)	0.129
Baseline Basophils, K/μL - median (IQR)	0.04 (0.04-0.04)	0.04 (0.04-0.04)	0.04 (0.04-0.04)	0.097
Baseline Hemoglobin, g/dL - median (IQR)	13.4 (12.95-14)	13.3 (12.7-14.15)	13.45 (13.17-13.67)	0.575
Low (<13.2) - no. (%)	8 (36.4)	5 (41.7)	3 (30.0)	0.263

Normal (13.2-16.4) - no. (%)	12 (54.5)	5 (41.7)	7 (70.0)	
Elevated (>16.4) - no. (%)	2 (9.1)	2 (16.7)	0 (0.0)	
Baseline Platelet Count, K/µL - median (IQR)	224.5 (187.75-253)	224 (171.75-251)	224.5 (208.25-268.75)	0.621
Normal (150-450) - no. (%)	21 (95.5)	11 (91.7)	10 (100.0)	1
Elevated (>450) - no. (%)	1 (4.5)	1 (8.3)	0 (0.0)	
Baseline D-dimer, µg/mL - median (IQR)	0.95 (0.58-1.92)	1.12 (0.69-1.65)	0.79 (0.45-1.82)	0.276
Normal (<0.50) - no. (%)	5 (22.7)	1 (8.3)	4 (40.0)	0.21
Elevated (≥0.50) - no. (%)	17 (77.3)	11 (91.7)	6 (60.0)	
Baseline International Normalized Ratio, sec - median (IQR)	1.1 (1-1.1)	1.1 (1-1.15)	1.1 (1-1.1)	0.487
Normal (0.9-1.1) - no. (%)	17 (77.3)	9 (75.0)	8 (80.0)	1
Elevated (>1.1) - no. (%)	5 (22.7)	3 (25.0)	2 (20.0)	
Baseline ESR, mm/hr - median (IQR)	51.5 (40-71)	43 (35.75-61.5)	64.5 (43.75-71)	0.198
Baseline CRP, mg/L - median (IQR)	80.59 (68.91-142.69)	80.59 (67.83-147.37)	90.22 (72.53-132.12)	0.895
Baseline Troponin, ng/mL - median (IQR)	0.01 (0.01-0.02)	0.01 (0.01-0.01)	0.01 (0.01-0.03)	0.193
Time from symptom onset to infusion, days - median (IQR)	10.5 (8.25-12.75)	10.5 (8.75-13)	10.5 (8.25-11)	0.571
Earlier (≤10) - no. (%)	11 (50.0)	6 (50.0)	5 (50.0)	1
Later (>10) - no. (%)	11 (50.0)	6 (50.0)	5 (50.0)	
Time from infusion to discharge, days - median (IQR)	6 (4-8.75)	6 (3.75-9)	5.5 (4-7.5)	0.618
Shorter (≤7) - no. (%)	15 (68.2)	8 (66.7)	7 (70.0)	1
Longer (>7) - no. (%)	7 (31.8)	4 (33.3)	3 (30.0)	
Total hospital stay, days - median (IQR)	9 (6-11.75)	9.5 (7.5-12.25)	7 (6-10)	0.371
Shorter (≤10) - no. (%)	15 (68.2)	7 (58.3)	8 (80.0)	0.531
Longer (>10) - no. (%)	7 (31.8)	5 (41.7)	2 (20.0)	
O_2 requirement at admission, L/min - median (IQR)	2 (2-4)	2 (2-8)	2.5 (2-3.25)	0.601
None (<1) - no. (%)	5 (22.7)	3 (25.0)	2 (20.0)	0.598
Low (1-49) - no. (%)	16 (72.7)	8 (66.7)	8 (80.0)	
High (≥50) - no. (%)	1 (4.5)	1 (8.3)	0 (0.0)	
Peak O_2 requirement during hospital stay, L/min - median (IQR)	6.5 (3.25-11.25)	8.5 (4.5-26.25)	5 (3.25-6.75)	0.119
Low (1-49) - no. (%)	18 (81.8)	9 (75.0)	9 (90.0)	0.724
High (≥50) - no. (%)	4 (18.2)	3 (25.0)	1 (10.0)	
O_2 requirement at discharge, L/min - median (IQR)	3 (3-3)	3 (3-3)	3 (2-3)	0.414
None (<1) - no. (%)	17 (77.3)	10 (83.3)	7 (70.0)	0.816
Low (1-49) - no. (%)	5 (22.7)	2 (16.7)	3 (30.0)	
ICU Stay - no. (%)	5 (22.7)	4 (33.3)	1 (10.0)	0.43
d) Concomitant Medication				
Concurrent COVID-19 Treatments - no. (%)				
Convalescent Plasma	19 (86.4)	10 (83.3)	9 (90.0)	1
Remdesivir	19 (86.4)	11 (91.7)	8 (80.0)	0.865
Dexamethasone	15 (68.2)	9 (75.0)	6 (60.0)	0.77
Anti-microbials	16 (72.7)	9 (75.0)	7 (70.0)	1

Median and Inter-quartile range (IQR) was determined for all continuous variables. P-values were obtained using Kruskal Wallis test continuous variables. Chi-square test was used to obtain p-values for categorical variables.

Table S2. Immune Cell Marker Panels.

Cytek Flow Cytometry Panel	
Marker	**Description**
CD45RA	BUV395 Mouse Anti-Human CD45RA
Viability dye	LIVE/DEAD™ Fixable Blue Dead Cell Stain Kit, for UV excitation
CD16	BUV496 Mouse Anti-Human CD16
CCR5	BUV563 Mouse Anti-Human CD195 (CCR5)
CD11c	BUV661 Mouse Anti-Human CD11c
CD56	BUV737 Mouse Anti-Human CD56
CD8	BD Horizon™ BUV805 Mouse Anti-Human CD8
CCR7	Brilliant Violet 421™ anti-human CD197 (CCR7) Antibody
CD123	CD123 Monoclonal Antibody (6H6), Super Bright 436, eBioscience™
CD161	CD161 Monoclonal Antibody (HP-3G10), eFluor 450, eBioscience™
IgD	BV480 Mouse Anti-Human IgD
CD3	Brilliant Violet 510™ anti-human CD3 Antibody
CD20	CD20 Monoclonal Antibody (HI47), Pacific Orange
IgM	Brilliant Violet 570™ anti-human IgM Antibody
IgG	BD Horizon™ BV605 Mouse Anti-Human IgG
CD28	Brilliant Violet 650™ anti-human CD28 Antibody (clone CD28.2)
CCR6	Brilliant Violet 711™ anti-human CD196 (CCR6) Antibody
CXCR5	BV750 Rat Anti-Human CXCR5 (CD185)
PD-1	Brilliant Violet 785™ anti-human CD279 (PD-1) Antibody
CD141	BD Horizon™ BB515 Mouse Anti-Human CD141
CD57	FITC anti-human CD57 Antibody
CD14	Spark Blue™ 550 anti-human CD14 Antibody
CD45	CD45 Monoclonal Antibody (H130), PerCP
CD11b	PerCP/Cyanine5.5 anti-human CD11b Antibody
TCR gd	TCR gamma/delta Monoclonal Antibody (B1.1), PerCP-eFluor 710, eBioscience™
CD25	CD25 Monoclonal Antibody (BC96), PE, eBioscience™
CD4	cFluor 568 Anti-human CD4
CD24	CD24 Monoclonal Antibody (eBioSN3 (SN3 A5-2H10)), PE-eFluor 610, eBioscience™
CD95	CD95 (APO-1/Fas) Monoclonal Antibody (DX2), PE-Cyanine5, eBioscience™
CXCR3	CD183 (CXCR3) Monoclonal Antibody (CEW33D), PE-Cyanine7, eBioscience™
CD27	CD27 Monoclonal Antibody (O323), APC, eBioscience™
CD1c	Alexa Fluor® 647 anti-human CD1c Antibody
CD19	Spark NIR™ 685 anti-human CD19 Antibody
CD127	APC-R700 Mouse Anti-Human CD127
HLA-DR	HLA-DR Monoclonal Antibody (L243), APC-eFluor 780, eBioscience™
CD38	CD38 APC-Fire810
Immune Monitoring Cytometry Panel	
Marker	**Description**
Viability dye	LIVE/DEAD™ Fixable Blue Dead Cell Stain Kit, for UV excitation
CD45	CD45 Monoclonal Antibody (2D1), Super Bright 645, eBioscience™
CD3	BUV395 Mouse Anti-Human CD3 Clone SK7
CD8	CD8a Monoclonal Antibody (OKT8 (OKT-8)), Super Bright 436, eBioscience™
CD4	CD4 Monoclonal Antibody (RPA-T4), PerCP-Cyanine5.5, eBioscience™
FOXP3	FOXP3 Monoclonal Antibody (PCH101), eFluor 450, eBioscience™
CD11b	BUV661 Rat Anti-CD11b Clone M1/70
CD56	Brilliant Violet 750™ anti-human CD56 (NCAM) Antibody
CD45RO	BB515 Mouse Anti-Human CD45RO Clone UCHL1
CD25	CD25 Monoclonal Antibody (BC96), Super Bright 600, eBioscience™
PD1	BUV737 Mouse Anti-Human CD279 (PD-1) Clone EH12.1
Tim3	CD366 (TIM3) Monoclonal Antibody (F38-2E2), Super Bright 702, eBioscience™
TOX	TOX Antibody, anti-human/mouse, APC, REAfinity™
TCF1	PE anti-TCF1 (TCF7) Antibody
CD44	APC/Cyanine7 anti-mouse/human CD44 Antibody
CD62L	BV421 Mouse Anti-Human CD62L Clone DREG-56
CTLA4	PE/Dazzle™ 594 anti-human CD152 (CTLA-4) Antibody
Lag-3	CD223 (LAG-3) Monoclonal Antibody (3DS223H), PE-Cyanine5, eBioscience™
Klrg1	Brilliant Violet 510™ anti-mouse/human KLRG1 (MAFA) Antibody
T-bet	BV786 Mouse Anti-T-bet Clone O4-46
Ki-67	Ki-67 Monoclonal Antibody (SolA15), PerCP-eFluor 710, eBioscience™
GzmB	Granzyme B Monoclonal Antibody (N4TL33), Alexa Fluor 532, eBioscience™
VISTA	VISTA Monoclonal Antibody (B7H5DS8), PE-Cyanine7, eBioscience™
ICOS	Alexa Fluor® 488 anti-human/mouse/rat CD278 (ICOS) Antibody

CD69	BUV805 Mouse Anti-Human CD69 Clone FN50

Table S3. First principal component (PC1) loadings of each activation marker were used as coefficients for defining the activation score.

Marker	PC1 loading for HD & COVID D1	Average Log-Fold Change (HD vs. COVID day 1)	Wilcoxon p-value (HD vs. COVID day 1)
CD8+ T cells			
T-bet	0.71	0.52	<0.001
Ki-67	0.39	0.46	<0.001
CD69	0.28	0.39	<0.001
TOX	0.40	0.31	<0.001
GZMB	0.31	0.20	<0.001
CD4+ T cells (total)			
T-bet	0.14	0.08	<0.001
Ki67	0.69	0.38	<0.001
CD69	0.34	0.41	<0.001
TOX	0.33	0.19	<0.001
PD1	0.53	0.11	<0.001
Treg cells			
Ki-67	0.76	0.33	<0.001
TOX	0.14	0.38	<0.001
CD25	0.07	0.09	<0.001
iCOS	0.43	0.17	<0.001
CTLA4	0.47	0.30	<0.001
NK cells			
TOX	0.16	0.42	<0.001
GZMB	0.07	0.28	<0.001
KLRG1	0.08	0.06	<0.001
Ki-67	0.89	0.84	<0.001
LAG3	0.03	0.08	<0.001

Table S4. Cytokine concentrations from plasma samples (pg/mL), as measured by multiplex ELISA.

Time point	Treatment	C-X-C Motif Chemokine Ligand 13 (CXCL13; BLC)	C-C Motif Chemokine Ligand 24 CCL24; (Eotaxin-2)	C-C Motif Chemokine Ligand 11 (CCL11; Eotaxin)	Granulocyte colony-stimulating factor (G-CSF)	Granulocyte- macrophage colony-stimulating factor (GM-CSF)	C-C Motif Chemokine Ligand 1 (CCL1; I-309)	Intercellular Adhesion Molecule 1 (ICAM-1)	Interleukin-4 (IL-4)
Day 1	Placebo	12.53	38.01	16.84	131.38	31.90	2.00	20527.30	1.01
Day 2	Placebo	4.70	49.97	23.44	41.96	139.30	2.00	29374.20	3.72
Day 4	Placebo	9.36	61.23	12.12	139.11	29.30	6.90	21762.90	0.10
Day 8	Placebo	3.99	60.31	27.20	0.00	105.70	2.50	22862.30	0.00
Day 1	Placebo	4.95	27.83	30.22	150.76	186.70	0.00	40216.90	0.00
Day 2	Placebo	5.08	36.44	24.41	0.00	75.70	0.60	31875.30	0.00
Day 4	Placebo	6.12	25.73	30.01	0.00	3.30	0.00	74582.80	0.00
Day 1	CD24Fc	12.53	8.96	37.60	27.61	36.90	4.20	22647.20	6.31
Day 2	CD24Fc	14.65	11.19	33.15	26.20	50.10	2.40	27288.00	1.54
Day 4	CD24Fc	14.74	29.21	42.24	10.47	142.60	6.30	63115.90	6.46
Day 1	Placebo	15.95	33.91	9.70	16.39	0.00	4.10	13311.00	0.00
Day 2	Placebo	21.36	64.68	11.42	46.54	0.00	6.20	49666.20	0.00
Day 4	Placebo	33.70	54.13	2.37	0.00	72.80	0.00	36863.20	0.00
Day 8	Placebo	1.21	82.72	8.57	21.50	9.00	0.00	34612.40	0.00
Day 1	CD24Fc	16.02	129.35	33.13	47.21	0.00	1.80	36471.50	0.00
Day 2	CD24Fc	11.50	73.40	24.00	41.07	0.00	0.80	27022.20	0.00
Day 4	CD24Fc	8.64	64.39	40.92	40.32	4.40	0.40	23973.70	0.00
Day 8	CD24Fc	6.74	38.32	43.17	1.47	12.90	0.10	15971.70	0.00
Day 1	CD24Fc	26.64	13.51	15.39	38.22	69.80	28.20	67829.20	0.00
Day 2	CD24Fc	31.75	12.59	4.43	32.61	43.50	11.80	55250.10	0.00
Day 4	CD24Fc	5.33	19.82	0.00	36.18	123.20	0.00	51403.20	0.00
Day 8	CD24Fc	13.06	25.65	27.53	30.73	82.00	5.30	74985.70	0.00
Day 1	Placebo	12.81	5.71	3.36	48.19	31.40	1.30	39761.20	0.00
Day 2	Placebo	18.12	8.31	7.13	50.62	23.30	16.10	53815.00	0.00
Day 4	Placebo	11.57	9.47	0.41	45.67	76.00	0.00	41634.80	0.00
Day 8	Placebo	5.83	9.57	0.27	39.26	0.00	0.00	28925.90	0.00
Day 1	CD24Fc	8.74	7.34	0.00	46.82	30.20	4.70	290257.10	0.00
Day 2	CD24Fc	6.24	9.55	2.51	51.98	0.00	48.30	161549.60	0.00
Day 4	CD24Fc	6.95	11.01	0.00	38.70	0.00	0.00	197095.10	0.00
Day 1	Placebo	23.72	15.20	11.60	28.44	20.90	11.30	50848.50	0.00
Day 2	Placebo	55.97	32.18	29.22	41.34	22.20	29.90	73935.60	0.00
Day 4	Placebo	27.66	17.79	19.14	35.25	0.00	0.00	73493.70	0.00
Day 1	CD24Fc	18.00	19.38	2.61	36.31	80.10	67.20	170861.50	0.00
Day 2	CD24Fc	38.94	11.05	11.85	47.34	13.70	32.30	440283.70	0.00
Day 4	CD24Fc	36.93	26.36	22.48	38.46	49.10	7.10	260565.90	0.00
Day 8	CD24Fc	10.31	24.25	42.22	42.16	2.70	19.10	125248.30	0.00
Day 1	CD24Fc	29.92	56.83	8.58	44.11	56.00	0.00	19834.40	0.00
Day 2	CD24Fc	21.76	125.06	26.44	24.38	23.30	0.00	12650.30	0.00
Day 4	CD24Fc	24.98	90.62	1.38	41.00	88.10	0.00	15490.60	0.00
Day 2	Placebo	25.81	97.58	14.79	38.49	19.70	0.00	641851.10	0.00
Day 1	CD24Fc	10.44	47.88	74.66	50.36	108.20	46.30	67385.40	0.00
Day 2	CD24Fc	10.41	50.73	104.94	65.76	108.60	39.40	90977.30	0.02

Time point	Treatment	C-X-C Motif Chemokine Ligand 13 (CXCL13; BLC)	C-C Motif Chemokine Ligand 24 CCL24; (Eotaxin-2)	C-C Motif Chemokine Ligand 11 (CCL11; Eotaxin)	Granulocyte colony-stimulating factor (G-CSF)	Granulocyte- macrophage colony-stimulating factor (GM-CSF)	C-C Motif Chemokine Ligand 1 (CCL1; I-309)	Intercellular Adhesion Molecule 1 (ICAM-1)	Interleukin-4 (IL-4)
Day 4	CD24Fc	12.84	36.01	0.00	42.07	92.70	17.70	62077.90	0.00
Day 1	Placebo	212.93	102.63	0.00	991.25	120.90	250.00	349107.40	162.94
Day 2	Placebo	66.59	67.11	378.70	539.39	103.10	193.60	291722.80	128.76
Day 4	Placebo	81.52	50.77	425.43	388.75	64.10	150.30	197747.80	59.66
Day 1	CD24Fc	22.75	15.40	181.44	50.45	18.30	0.00	139448.60	0.00
Day 2	CD24Fc	20.08	23.07	263.20	61.25	0.00	0.00	146635.70	0.00
Day 4	CD24Fc	12.12	26.31	154.88	50.49	64.50	10.60	127301.30	0.00
Day 1	Placebo	25.02	11.76	98.97	42.80	9.40	0.00	229209.90	0.00
Day 2	Placebo	15.25	12.56	77.88	33.60	85.40	0.00	210878.20	0.00
Day 4	Placebo	9.67	10.19	134.79	32.97	56.40	0.00	707097.60	0.00
Day 1	CD24Fc	33.56	30.13	205.87	41.78	110.90	0.00	620242.10	0.00
Day 2	CD24Fc	27.79	34.17	106.16	83.03	39.90	0.00	644971.80	0.00
Day15	CD24Fc	14.24	30.70	80.51	147.72	50.00	65.20	711227.80	0.00
Day 1	Placebo	60.29	53.19	362.63	309.77	60.50	254.40	229168.10	98.69
Day 2	Placebo	69.81	61.30	535.30	641.33	173.00	205.20	173863.70	145.39
Day 4	Placebo	82.70	38.03	441.94	521.90	212.80	203.80	369359.70	91.22
Day 1	CD24Fc	60.65	52.30	293.53	273.07	121.80	107.50	232616.20	44.19
Day 2	CD24Fc	68.26	34.69	259.84	285.05	68.50	69.90	222667.00	36.54
Day 4	CD24Fc	51.75	63.70	448.67	288.45	88.70	76.50	244856.10	62.31
Day 1	Placebo	51.60	40.98	353.32	171.15	309.90	115.90	128269.60	26.70
Day 2	Placebo	47.86	40.39	292.81	186.55	155.50	91.90	269854.80	34.13
Day 4	Placebo	58.43	66.92	473.94	425.67	238.70	196.50	245009.70	115.88
Day 8	Placebo	45.88	62.25	431.67	228.11	120.50	127.80	179736.00	35.32
Day 1	Placebo	175.78	25.01	507.55	69.75	60.40	38.50	642359.80	0.00
Day 2	Placebo	157.93	23.21	127.47	108.44	22.50	44.70	596807.60	0.00
Day 4	Placebo	190.30	52.90	475.43	102.31	54.20	66.00	915164.70	0.00
Day 8	Placebo	310.85	49.00	59.70	65.06	37.60	32.00	427184.20	0.00
Day15	Placebo	152.21	60.45	364.89	52.93	0.00	35.70	696071.90	0.00
Day 1	Placebo	18.46	66.15	93.38	68.93	5.30	0.00	66878.10	0.00
Day 2	Placebo	16.50	61.55	165.76	66.31	31.20	0.00	111900.60	0.00
	Healthy Donors	4.53	151.36	20.01	1072.96	55.87	1.06	15963.72	0.95
	Healthy Donors	14.96	133.09	33.10	159.53	133.13	0.95	27944.49	1.86
	Healthy Donors	6.98	121.76	31.71	135.36	121.45	1.49	30490.73	0.08
	Healthy Donors	10.10	30.07	23.79	1004.70	309.67	1.78	37735.78	5.39
	Healthy Donors	1.61	480.40	9.65	0.00	79.88	0.00	144172.30	0.00
	Healthy Donors	1.27	252.17	9.92	0.00	180.45	0.00	199822.17	0.00
	Healthy Donors	3.74	196.21	15.30	13.47	61.60	0.41	146682.40	0.00
	Healthy Donors	3.48	628.34	27.68	0.00	137.50	0.00	102571.91	0.00
	Healthy Donors	1.47	430.58	8.63	0.00	271.14	0.00	2324.59	0.00
	Healthy Donors	9.84	151.00	15.17	29.21	856.48	1.06	15426.11	0.00
	Healthy Donors	0.00	203.38	36.57	0.00	327.04	0.00	16919.45	0.00
	Healthy Donors	0.00	84.90	19.55	0.00	382.48	0.00	15233.18	0.00
	Healthy Donors	4.59	30.40	4.76	0.00	25.67	2.04	129264.72	1.52
	Healthy Donors	3.54	207.55	21.12	70.90	0.00	0.00	359668.97	0.00

Time point	Treatment	C-X-C Motif Chemokine Ligand 13 (CXCL13; BLC)	C-C Motif Chemokine Ligand 24 CCL24; (Eotaxin-2)	C-C Motif Chemokine Ligand 11 (CCL11; Eotaxin)	Granulocyte colony-stimulating factor (G-CSF)	Granulocyte- macrophage colony-stimulating factor (GM-CSF)	C-C Motif Chemokine Ligand 1 (CCL1; I-309)	Intercellular Adhesion Molecule 1 (ICAM-1)	Interleukin-4 (IL-4)
	Healthy Donors	1.38	13.06	1.57	0.00	0.00	0.02	7440.88	0.00
	Healthy Donors	1.22	69.56	21.64	10.88	0.00	0.00	13929.65	5.46
	Healthy Donors	3.20	45.96	19.06	0.00	0.00	0.09	6787.48	0.00
	Healthy Donors	12.17	10.64	80.37	0.00	0.00	0.00	13113.68	0.00
	Healthy Donors	20.45	40.33	30.38	302.95	0.00	0.70	24719.27	5.14
	Healthy Donors	11.94	47.78	77.22	26.06	0.00	0.48	87587.09	2.10
	Healthy Donors	124.66	12.61	61.46	0.00	53.95	0.00	229829.81	0.26
	Healthy Donors	14.03	43.16	40.21	0.00	15.91	1.40	11284.43	0.00
	Healthy Donors	56.10	149.29	56.65	482.73	0.33	9.25	55734.14	17.49
	Healthy Donors	28.94	39.20	56.10	469.04	416.95	20.78	22217.29	16.60
	Healthy Donors	5.82	89.46	46.37	0.00	0.00	0.00	8137.58	0.00

Time point	Treatment	Interleukin-10 (IL-10)	Interleukin-12 subunit p40 (IL-12p40)	Interleukin-15 (IL-15)	Interleukin-16 (IL-16)	Interleukin-1 alpha (IL-1a)	Interleukin-1 beta (IL-1b)	Interleukin-5 (IL-5)	Interleukin-6 (IL-6)
Day 1	Placebo	5.04	57.47	110.71	179.85	45.20	4.72	4.98	14.49
Day 2	Placebo	12.07	77.95	792.67	344.96	78.70	4.99	84.24	15.94
Day 4	Placebo	7.35	34.20	399.70	381.20	51.90	4.17	123.92	42.52
Day 8	Placebo	17.01	0.00	425.84	460.11	173.00	3.58	360.18	34.15
Day 1	Placebo	2.57	35.92	0.00	0.00	117.10	0.00	342.24	26.58
Day 2	Placebo	11.29	30.77	23.25	20.96	124.30	2.57	217.49	22.52
Day 4	Placebo	1.71	54.96	13.82	0.00	31.00	1.09	17.89	12.30
Day 1	CD24Fc	5.02	43.96	35.67	44.67	8.60	3.02	65.54	21.30
Day 2	CD24Fc	0.00	87.50	0.00	0.00	34.60	2.53	60.49	15.53
Day 4	CD24Fc	9.55	131.74	79.82	45.67	112.20	1.72	177.87	36.13
Day 1	Placebo	0.24	24.36	0.00	0.00	34.10	2.61	20.23	16.39
Day 2	Placebo	1.26	28.07	0.00	0.00	17.30	2.46	0.00	16.18
Day 4	Placebo	5.39	2.32	0.00	0.00	98.60	0.90	109.87	13.37
Day 8	Placebo	0.99	0.00	11.10	1.95	84.10	2.52	0.00	8.10
Day 1	CD24Fc	0.00	115.44	29.72	36.01	22.70	3.59	0.00	6.63
Day 2	CD24Fc	0.00	102.15	0.00	51.55	0.00	3.42	0.00	5.45
Day 4	CD24Fc	0.00	41.45	19.63	106.01	52.30	3.32	4.82	6.59
Day 8	CD24Fc	0.00	0.00	0.00	70.09	47.00	2.76	14.34	9.35
Day 1	CD24Fc	0.00	27.29	132.54	134.83	15.70	1.77	498.34	17.64
Day 2	CD24Fc	0.00	8.73	94.58	44.60	14.00	1.71	593.45	35.87
Day 4	CD24Fc	0.00	0.00	113.57	145.38	11.50	0.60	739.84	11.62
Day 8	CD24Fc	0.00	0.00	73.29	102.09	14.10	1.40	749.68	6.11
Day 1	Placebo	0.00	422.32	95.59	321.82	26.60	11.10	770.09	1.44
Day 2	Placebo	0.00	489.92	108.85	339.16	15.00	11.22	80.00	2.55
Day 4	Placebo	0.00	277.43	132.62	493.83	26.30	13.28	358.06	0.94
Day 8	Placebo	0.00	109.07	65.93	167.25	13.20	3.10	391.03	0.00
Day 1	CD24Fc	28.74	23.87	181.89	194.04	46.40	2.42	654.26	11.71
Day 2	CD24Fc	0.00	20.16	239.89	246.40	36.80	7.60	0.00	2.66
Day 4	CD24Fc	0.00	83.61	86.80	94.16	15.90	0.81	2.64	0.00
Day 1	Placebo	0.00	0.00	37.14	0.00	0.00	0.66	0.00	0.75
Day 2	Placebo	0.00	10.24	105.57	57.61	0.00	0.00	179.76	0.72
Day 4	Placebo	0.00	7.05	67.42	155.70	1.80	0.34	0.00	4.79
Day 1	CD24Fc	0.00	24.45	259.36	161.49	22.10	2.09	580.68	21.33
Day 2	CD24Fc	0.00	38.92	103.60	80.27	32.80	0.00	0.00	0.00
Day 4	CD24Fc	0.00	0.00	105.04	172.00	33.00	0.94	112.43	9.91
Day 8	CD24Fc	0.00	0.36	71.59	20.45	0.00	0.66	0.00	0.00
Day 1	CD24Fc	0.00	7.38	90.76	21.03	17.80	3.18	5.85	4.05
Day 2	CD24Fc	0.00	0.00	50.25	20.29	53.70	0.79	115.41	10.60
Day 4	CD24Fc	0.00	0.00	30.12	18.82	26.40	2.73	397.68	8.31
Day 2	Placebo	1.67	0.00	73.34	138.95	31.10	2.90	988.77	2.44
Day 1	CD24Fc	13.22	32.19	404.26	1317.19	75.10	1.88	407.41	22.79
Day 2	CD24Fc	0.00	93.64	524.95	1233.54	66.30	3.94	113.51	18.36

Time point	Treatment	Interleukin-10 (IL-10)	Interleukin-12 subunit p40 (IL-12p40)	Interleukin-15 (IL-15)	Interleukin-16 (IL-16)	Interleukin-1 alpha (IL-1a)	Interleukin-1 beta (IL-1b)	Interleukin-5 (IL-5)	Interleukin-6 (IL-6)
Day 4	CD24Fc	0.00	0.00	255.28	952.11	39.10	1.92	396.98	7.07
Day 1	Placebo	22.77	37178.56	1597.54	4882.12	771.30	227.72	7524.20	73.85
Day 2	Placebo	31.89	21647.52	1945.67	4466.37	454.60	148.97	2927.77	59.19
Day 4	Placebo	0.03	23032.62	1559.13	3638.09	476.30	118.74	3590.32	40.15
Day 1	CD24Fc	0.00	1491.20	132.89	234.19	80.80	12.00	0.00	4.76
Day 2	CD24Fc	0.00	4091.56	99.45	275.23	112.90	12.15	0.00	0.78
Day 4	CD24Fc	0.00	312.59	69.92	121.40	102.70	8.20	83.26	3.83
Day 1	Placebo	0.00	12.18	68.87	152.57	52.70	1.40	0.00	3.65
Day 2	Placebo	0.00	0.00	62.23	147.30	69.60	0.00	377.70	8.88
Day 4	Placebo	0.00	0.79	70.51	139.51	72.50	1.90	0.00	8.70
Day 1	CD24Fc	19.07	78.84	184.90	394.18	211.80	1.73	1209.78	37.07
Day 2	CD24Fc	0.00	31.71	79.91	243.93	126.90	8.02	284.37	17.26
Day15	CD24Fc	0.00	421.70	239.17	598.91	52.50	13.46	563.19	17.10
Day 1	Placebo	0.61	768.23	332.44	2270.59	611.60	89.91	1656.84	96.64
Day 2	Placebo	4.61	7973.43	632.57	2845.82	596.50	70.30	3226.78	36.03
Day 4	Placebo	32.38	3451.02	628.62	2064.34	518.70	95.12	2670.52	37.24
Day 1	CD24Fc	0.00	6700.21	1627.10	3963.42	181.90	74.39	2643.06	24.93
Day 2	CD24Fc	0.00	6805.71	1438.39	3551.34	145.40	80.75	2082.17	12.76
Day 4	CD24Fc	0.00	13685.95	923.52	3144.59	217.90	83.97	1950.27	12.66
Day 1	Placebo	57.75	4287.19	1302.02	2700.93	124.60	37.08	3993.91	11.68
Day 2	Placebo	25.62	17697.75	1352.06	2814.66	132.30	47.44	2752.12	12.29
Day 4	Placebo	28.56	19328.37	2644.53	6871.18	316.40	115.83	4201.80	14.05
Day 8	Placebo	5.97	13543.34	1402.82	3050.74	236.50	58.81	2658.04	10.78
Day 1	Placebo	2.70	1147.58	44.48	106.52	73.20	2.27	585.94	0.00
Day 2	Placebo	0.00	400.54	45.51	44.20	61.60	2.37	572.38	0.00
Day 4	Placebo	5.18	882.55	68.93	91.74	72.70	2.82	700.86	12.77
Day 8	Placebo	0.00	250.08	74.54	81.14	34.20	1.73	229.50	0.00
Day15	Placebo	0.00	90.02	81.88	119.01	35.00	0.97	0.00	2.06
Day 1	Placebo	0.00	2440.65	289.60	1209.38	62.50	13.67	692.24	0.00
Day 2	Placebo	16.07	1737.00	355.20	1778.69	92.80	11.01	1048.97	4.61
	Healthy Donors	0.89	110.57	408.35	606.70	10.92	0.90	272.89	5.56
	Healthy Donors	6.11	0.00	380.21	196.70	18.54	0.61	609.16	14.38
	Healthy Donors	5.29	36.10	243.74	23.40	13.20	0.00	414.93	16.46
	Healthy Donors	9.59	152.23	1694.47	2142.97	37.71	23.97	1476.23	40.58
	Healthy Donors	0.82	3.17	0.00	0.00	0.00	0.00	213.54	7.32
	Healthy Donors	1.67	0.00	0.00	0.00	0.00	0.00	993.26	11.72
	Healthy Donors	0.47	0.00	11.25	177.57	0.00	0.84	364.17	5.56
	Healthy Donors	1.84	74.42	384.33	2072.26	12.61	0.13	902.58	8.82
	Healthy Donors	2.29	2.50	64.55	289.43	15.84	0.00	836.45	4.62
	Healthy Donors	13.02	40.17	193.49	124.55	200.91	0.88	5272.42	84.67
	Healthy Donors	4.39	53.43	223.02	537.48	95.35	0.66	2140.58	50.69
	Healthy Donors	10.49	25.07	54.12	0.00	129.80	0.63	2850.94	42.03
	Healthy Donors	1.54	1.99	10.09	183.49	0.00	0.00	466.64	0.00
	Healthy Donors	0.00	21.76	0.00	0.00	0.00	0.00	0.00	0.00

Time point	Treatment	Interleukin-10 (IL-10)	Interleukin-12 subunit p40 (IL-12p40)	Interleukin-15 (IL-15)	Interleukin-16 (IL-16)	Interleukin-1 alpha (IL-1a)	Interleukin-1 beta (IL-1b)	Interleukin-5 (IL-5)	Interleukin-6 (IL-6)
	Healthy Donors	0.00	0.00	0.00	0.00	0.00	1.44	0.00	0.00
	Healthy Donors	0.00	103.39	275.57	1268.58	0.00	8.25	0.00	0.00
	Healthy Donors	1.55	0.00	0.00	171.11	0.00	1.05	0.00	0.00
	Healthy Donors	0.90	17.48	188.82	2009.51	0.00	0.32	193.87	0.00
	Healthy Donors	0.00	383.38	93.53	882.52	0.00	10.63	243.42	7.76
	Healthy Donors	0.52	0.00	10.00	237.42	25.83	1.70	0.00	4.99
	Healthy Donors	0.00	0.00	0.00	0.00	0.00	0.00	509.23	0.00
	Healthy Donors	0.00	1.25	0.00	0.00	0.00	0.00	272.40	0.00
	Healthy Donors	0.70	179.68	942.17	9316.17	255.23	24.62	1112.35	15.69
	Healthy Donors	7.08	798.03	660.17	3337.76	95.50	15.22	3552.43	49.12
	Healthy Donors	0.00	12.80	34.89	378.84	0.00	0.00	69.90	0.00

Time point	Treatment	Soluble IL-6 receptor (IL-6sR)	Interleukin-7 (IL-7)	Interleukin-8 (IL-8)	Macrophage colony-stimulating factor (M-CSF)	C-X-C Motif Chemokine Ligand 9 (CXCL9; MIG)	C-C Motif Chemokine Ligand 3 (CCL3; MIP-1a)	C-C Motif Chemokine Ligand 4 (CCL4; MIP-1b)	C-C Motif Chemokine Ligand 15 (CCL15; MIP-1d)
Day 1	Placebo	2541.47	0.00	4.14	0.00	16.94	129.67	13.00	1254.90
Day 2	Placebo	3335.06	47.52	14.73	0.00	7.64	233.88	22.45	4104.30
Day 4	Placebo	2602.15	26.65	23.45	0.00	18.89	387.03	21.55	299.50
Day 8	Placebo	2478.02	163.39	48.25	0.00	30.10	459.27	30.90	2105.10
Day 1	Placebo	2809.77	172.51	21.93	0.00	0.00	28.66	53.75	4576.90
Day 2	Placebo	3083.93	67.44	16.60	0.00	30.04	45.24	56.23	4219.30
Day 4	Placebo	3106.32	5.58	10.89	0.00	5.54	29.91	60.76	4679.70
Day 1	CD24Fc	2785.28	29.55	0.03	0.00	17.96	26.45	10.81	2055.90
Day 2	CD24Fc	2891.71	2.15	0.00	0.00	4.86	18.42	10.29	1973.80
Day 4	CD24Fc	3989.19	135.85	8.08	0.00	5.71	42.82	23.76	6277.40
Day 1	Placebo	2621.07	6.77	1.17	0.00	15.43	47.09	18.74	1328.40
Day 2	Placebo	2573.31	0.00	0.72	0.00	25.01	41.43	23.69	1724.30
Day 4	Placebo	3132.98	61.02	9.73	0.00	13.17	23.60	22.79	1994.40
Day 8	Placebo	3449.81	39.53	5.58	0.00	5.54	94.44	58.57	1608.50
Day 1	CD24Fc	2471.04	0.00	0.00	0.00	25.06	215.10	22.38	2198.90
Day 2	CD24Fc	1905.90	0.00	0.81	0.00	22.68	152.94	13.52	1218.50
Day 4	CD24Fc	2590.94	13.00	2.67	0.00	22.97	195.81	23.11	1233.80
Day 8	CD24Fc	2399.09	5.02	0.00	0.00	8.60	133.38	22.13	377.60
Day 1	CD24Fc	2316.94	0.00	0.00	267.10	0.00	47.67	26.84	3870.50
Day 2	CD24Fc	2165.96	0.00	0.00	44.14	0.00	51.58	39.45	5321.00
Day 4	CD24Fc	2097.89	5.31	0.00	111.40	195.95	61.35	37.31	2318.40
Day 8	CD24Fc	2182.06	0.00	0.00	89.17	58.09	82.88	101.26	2064.90
Day 1	Placebo	2234.59	0.00	0.00	91.43	492.69	121.86	33.98	1861.90
Day 2	Placebo	2241.69	0.00	0.00	48.03	419.01	99.22	48.68	1544.30
Day 4	Placebo	898.48	0.27	0.00	129.60	249.44	101.88	43.46	1788.90
Day 8	Placebo	1080.89	6.69	0.00	0.00	37.80	41.74	76.82	108.90
Day 1	CD24Fc	2886.11	0.00	29.15	560.79	59.77	21.97	20.99	932.40
Day 2	CD24Fc	2382.04	0.00	0.00	720.73	0.00	21.29	18.57	1917.10
Day 4	CD24Fc	2524.17	0.00	0.00	252.56	45.62	27.82	24.46	945.50
Day 1	Placebo	2664.03	0.00	0.00	70.78	7.72	18.60	11.07	3124.40
Day 2	Placebo	2153.58	0.00	0.00	186.44	0.00	19.91	7.68	626.60
Day 4	Placebo	2053.29	0.00	0.00	230.57	0.00	19.50	12.97	1915.40
Day 1	CD24Fc	2440.25	1.20	0.00	115.46	6.38	32.73	35.52	869.10
Day 2	CD24Fc	2474.51	0.00	0.00	292.29	0.00	7.20	17.39	2776.90
Day 4	CD24Fc	2035.68	0.00	0.00	0.00	0.00	13.24	19.18	849.10
Day 8	CD24Fc	2339.47	0.00	0.00	27.34	11.03	24.09	33.03	842.00
Day 1	CD24Fc	2301.31	0.00	0.00	0.00	0.00	11.61	17.07	728.60
Day 2	CD24Fc	2767.73	0.00	0.00	0.00	0.00	11.68	17.32	1471.70
Day 4	CD24Fc	2354.02	0.20	0.00	134.22	2.57	8.76	13.03	661.40
Day 2	Placebo	1774.96	1.90	0.00	140.92	0.00	23.00	29.49	2545.90
Day 1	CD24Fc	2220.69	17.70	120.71	0.00	0.00	19.37	21.43	1060.90
Day 2	CD24Fc	3321.08	0.00	168.33	0.00	0.00	8.56	12.66	1116.50

Time point	Treatment	Soluble IL-6 receptor (IL-6sR)	Interleukin-7 (IL-7)	Interleukin-8 (IL-8)	Macrophage colony-stimulating factor (M-CSF)	C-X-C Motif Chemokine Ligand 9 (CXCL9; MIG)	C-C Motif Chemokine Ligand 3 (CCL3; MIP-1a)	C-C Motif Chemokine Ligand 4 (CCL4; MIP-1b)	C-C Motif Chemokine Ligand 15 (CCL15; MIP-1d)
Day 4	CD24Fc	2479.81	0.00	55.65	24.47	0.00	20.82	23.06	1362.90
Day 1	Placebo	3773.12	129.76	361.18	5177.57	4352.43	662.83	51.75	51847.20
Day 2	Placebo	3417.72	33.22	387.85	2072.01	4940.86	428.79	34.17	27788.50
Day 4	Placebo	2362.03	95.65	249.22	1799.73	4694.05	672.03	38.25	44491.90
Day 1	CD24Fc	2308.57	0.00	0.00	5.40	43.10	18.51	30.04	2686.90
Day 2	CD24Fc	2606.61	0.00	0.00	6.72	80.85	26.14	16.12	9537.50
Day 4	CD24Fc	2912.73	0.04	0.00	7.25	45.13	18.78	31.37	2448.20
Day 1	Placebo	1900.17	0.00	0.00	110.88	0.00	4.50	14.01	3197.40
Day 2	Placebo	2086.75	8.39	0.00	54.35	0.84	3.47	11.44	702.50
Day 4	Placebo	2425.20	0.00	0.00	173.22	0.64	6.53	20.13	723.20
Day 1	CD24Fc	2265.89	52.76	55.17	0.00	97.03	14.45	51.40	5328.30
Day 2	CD24Fc	2055.71	9.39	12.05	0.00	25.83	36.39	61.25	1796.30
Day15	CD24Fc	2773.70	0.36	11.10	79.33	199.51	155.10	83.73	3639.80
Day 1	Placebo	2549.27	26.73	60.08	72.26	570.92	26.71	44.36	10581.70
Day 2	Placebo	2587.47	49.21	50.95	0.00	325.84	2.30	21.76	13403.40
Day 4	Placebo	2758.12	72.87	88.42	233.97	521.78	9.15	34.68	14929.60
Day 1	CD24Fc	2812.93	82.12	153.85	422.05	1241.49	344.53	36.55	13969.40
Day 2	CD24Fc	3048.03	11.14	62.80	425.29	840.59	422.33	14.91	37941.40
Day 4	CD24Fc	3149.08	38.24	129.80	721.95	1351.04	326.28	36.94	59747.70
Day 1	Placebo	2476.94	182.98	218.43	2142.73	679.38	245.74	71.61	19943.00
Day 2	Placebo	3011.33	134.27	148.09	2359.22	3082.49	513.67	67.89	26598.90
Day 4	Placebo	3259.70	180.27	218.67	4404.95	1098.19	331.51	86.20	47446.30
Day 8	Placebo	2734.89	96.49	176.09	783.85	819.96	257.76	113.24	23748.10
Day 1	Placebo	3291.55	3.22	0.00	349.80	178.18	77.95	24.70	21238.80
Day 2	Placebo	3024.38	0.00	0.00	0.00	91.84	94.03	39.53	8439.20
Day 4	Placebo	2751.91	8.06	0.00	165.12	151.81	180.96	108.68	15952.00
Day 8	Placebo	2489.04	0.00	0.00	0.00	85.26	110.43	60.03	29803.70
Day15	Placebo	3065.14	0.00	3.98	0.00	99.61	107.61	43.24	13205.10
Day 1	Placebo	3075.81	2.77	12.02	33.88	861.42	104.45	25.73	6232.20
Day 2	Placebo	2875.38	5.96	25.51	34.09	551.42	27.23	23.24	9051.40
	Healthy Donors	924.97	26.50	48.98	377.94	117.88	45.03	35.91	1649.93
	Healthy Donors	880.46	81.84	107.11	358.76	1.73	8.61	9.31	241.87
	Healthy Donors	1183.67	71.00	98.13	0.00	0.00	8.81	7.33	338.39
	Healthy Donors	870.17	128.82	251.12	0.00	28.12	53.58	21.38	1358.02
	Healthy Donors	876.14	32.16	15.80	140.30	0.00	4.58	10.39	189.23
	Healthy Donors	736.57	61.41	50.88	19.11	0.00	5.65	14.46	543.38
	Healthy Donors	879.22	0.00	15.55	37.23	3.14	12.05	32.45	185.35
	Healthy Donors	924.36	57.12	107.54	0.00	3.69	35.71	25.43	98.13
	Healthy Donors	445.54	48.49	58.11	135.13	0.00	0.00	27.18	0.00
	Healthy Donors	815.79	240.57	391.96	0.00	0.00	24.60	22.59	0.00
	Healthy Donors	891.47	104.09	208.17	0.00	15.27	61.48	9.48	279.15
	Healthy Donors	1128.42	127.86	315.47	61.40	0.00	3.43	58.69	3516.90
	Healthy Donors	1479.76	0.00	69.99	0.00	0.00	30.96	24.77	188.59
	Healthy Donors	872.89	0.00	0.00	0.00	0.00	4.12	15.21	784.58

Time point	Treatment	Soluble IL-6 receptor (IL-6sR)	Interleukin-7 (IL-7)	Interleukin-8 (IL-8)	Macrophage colony-stimulating factor (M-CSF)	C-X-C Motif Chemokine Ligand 9 (CXCL9; MIG)	C-C Motif Chemokine Ligand 3 (CCL3; MIP-1a)	C-C Motif Chemokine Ligand 4 (CCL4; MIP-1b)	C-C Motif Chemokine Ligand 15 (CCL15; MIP-1d)
	Healthy Donors	706.76	0.00	0.00	0.00	5.71	0.00	2.05	254.75
	Healthy Donors	869.17	0.00	0.00	0.00	76.33	108.12	6.44	2222.22
	Healthy Donors	1252.18	0.00	72.26	0.00	14.49	0.95	6.12	283.42
	Healthy Donors	970.05	23.03	159.10	1429.42	102.73	17.85	21.67	548.15
	Healthy Donors	1260.67	17.41	58.89	39.12	96.04	26.30	7.81	1114.14
	Healthy Donors	1092.99	0.00	55.86	121.57	24.32	9.86	6.62	105.71
	Healthy Donors	1007.40	8.88	26.96	6.21	8.04	0.00	8.57	2346.87
	Healthy Donors	749.62	5.11	0.00	0.00	27.65	7.89	6.99	143.60
	Healthy Donors	1205.72	27.00	218.24	1130.81	47.08	87.70	17.94	2750.50
	Healthy Donors	934.42	122.46	285.51	387.87	434.56	240.63	29.83	5092.84
	Healthy Donors	1067.04	4.02	0.00	10.35	0.00	17.71	13.37	1115.47

Time point	Treatment	Platelet- Derived Growth Factor-BB (PDGF-BB)	C-C Motif Chemokine Ligand 5 (CCL5; RANTES)	Tissue Inhibitor Of Metallo-proteinases-1 (TIMP-1)	Tissue Inhibitor Of Metallo-proteinases-2 (TIMP-2)	Tumor Necrosis Factor Receptor Superfamily, Member 1A (TNFRSF1A; TNF RI)	Tumor Necrosis Factor Receptor Superfamily, Member 1B (TNFRSF1B; TNF RII)
Day 1	Placebo	1712.90	2662.73	14990.50	80339.00	2284.05	9067.98
Day 2	Placebo	10453.90	4940.83	49765.30	364467.90	2874.63	3032.09
Day 4	Placebo	1491.80	3457.51	3712.10	197.20	988.77	5978.24
Day 8	Placebo	22560.00	5469.92	46604.00	210741.40	2399.16	14437.05
Day 1	Placebo	20248.80	5851.85	7075.30	1146.70	1262.17	6946.09
Day 2	Placebo	19206.20	5818.02	18887.30	39420.20	1473.69	10053.14
Day 4	Placebo	15212.50	5322.38	533.50	224.00	1879.92	9997.14
Day 1	CD24Fc	1796.40	5187.36	1467.90	2755.50	1914.64	8347.28
Day 2	CD24Fc	5273.70	5401.22	19618.80	6713.80	2059.34	8432.03
Day 4	CD24Fc	10414.40	6708.13	7845.90	2431.40	2324.90	9290.60
Day 1	Placebo	6147.10	5637.95	25572.20	435.90	2122.44	10567.47
Day 2	Placebo	2047.80	4470.85	4913.50	4430.70	1850.34	4491.54
Day 4	Placebo	12469.30	6759.29	11551.20	503.20	1707.65	8336.14
Day 8	Placebo	9985.00	6914.88	45782.60	65254.60	1397.21	7236.14
Day 1	CD24Fc	1329.40	1784.06	10271.80	48435.50	213.73	5568.67
Day 2	CD24Fc	1200.10	1924.88	11861.70	693.50	11.87	4679.09
Day 4	CD24Fc	7941.70	4642.62	28583.60	18068.40	65.71	6043.11
Day 8	CD24Fc	6954.00	3937.45	27105.10	56096.10	0.00	7070.57
Day 1	CD24Fc	814.90	2818.80	49190.60	94836.70	3308.46	8564.99
Day 2	CD24Fc	1830.00	3617.18	25657.20	87438.40	3243.79	9988.40
Day 4	CD24Fc	2201.00	4902.98	32371.80	119201.20	2730.09	10919.83
Day 8	CD24Fc	3708.10	6814.33	71836.90	130696.10	3619.17	14657.63
Day 1	Placebo	1540.70	3580.72	15458.20	51039.80	2099.70	8175.95
Day 2	Placebo	517.30	1844.82	16979.80	68238.90	1876.45	9334.78
Day 4	Placebo	954.70	2366.34	19144.00	101605.90	1090.47	7217.97
Day 8	Placebo	468.00	3234.22	28576.70	67539.30	950.54	8047.54
Day 1	CD24Fc	3835.40	8861.67	33663.60	211024.50	3252.77	11150.23
Day 2	CD24Fc	2282.10	6944.81	53063.30	100413.30	3470.95	7289.87
Day 4	CD24Fc	814.50	5512.46	63469.30	76147.80	4656.48	7568.75
Day 1	Placebo	802.50	4142.84	68286.60	91581.90	7648.48	9640.21
Day 2	Placebo	929.30	3508.18	41984.60	80789.40	5077.43	8440.94
Day 4	Placebo	1785.20	5493.27	70972.30	96202.70	6929.25	10669.81
Day 1	CD24Fc	4669.50	6319.63	57444.50	75939.20	2731.93	13173.35
Day 2	CD24Fc	8869.50	9124.68	60155.90	128527.80	2506.61	13809.00
Day 4	CD24Fc	1839.70	3051.75	46402.80	69536.50	2707.99	10963.95
Day 8	CD24Fc	1296.70	2531.85	42035.20	99801.00	1837.32	12749.85
Day 1	CD24Fc	1097.80	4873.53	24600.30	110692.30	2241.93	9421.65
Day 2	CD24Fc	4051.00	5677.44	80163.00	93559.70	3930.34	12426.17
Day 4	CD24Fc	1014.80	2896.65	34622.80	75032.70	1071.14	4355.35
Day 2	Placebo	4383.90	5907.06	79694.10	88210.90	2153.32	5242.79
Day 1	CD24Fc	3990.30	4401.15	52891.30	95849.50	4206.30	11629.83
Day 2	CD24Fc	1617.10	2320.00	81483.50	210791.80	5721.40	21517.60

Time point	Treatment	Platelet- Derived Growth Factor-BB (PDGF-BB)	C-C Motif Chemokine Ligand 5 (CCL5; RANTES)	Tissue Inhibitor Of Metallo-proteinases-1 (TIMP-1)	Tissue Inhibitor Of Metallo-proteinases-2 (TIMP-2)	Tumor Necrosis Factor Receptor Superfamily, Member 1A (TNFRSF1A; TNF RI)	Tumor Necrosis Factor Receptor Superfamily, Member 1B (TNFRSF1B; TNF RII)
Day 4	CD24Fc	1781.00	2637.90	33658.60	69731.00	3092.35	6344.70
Day 1	Placebo	22294.70	7943.34	77257.30	98779.20	16606.30	21050.80
Day 2	Placebo	19289.00	8000.49	63115.40	83648.00	10406.64	14463.86
Day 4	Placebo	25596.50	7421.00	67517.80	131694.40	11135.08	19547.59
Day 1	CD24Fc	2249.40	4776.96	58325.40	99065.10	4341.63	13676.10
Day 2	CD24Fc	6798.20	4376.98	45717.10	172048.70	4520.00	11281.50
Day 4	CD24Fc	2544.80	3265.93	50312.50	75939.50	2837.11	6972.59
Day 1	Placebo	4052.20	1790.83	58768.00	147179.10	1393.12	6284.92
Day 2	Placebo	6449.70	2413.88	43961.00	84587.30	1059.63	3918.37
Day 4	Placebo	15171.70	5017.50	62769.10	138164.20	1546.87	10814.97
Day 1	CD24Fc	21880.60	7262.22	94679.90	107856.90	2572.43	9774.89
Day 2	CD24Fc	15739.80	7461.52	89337.30	140213.70	1481.73	10659.60
Day15	CD24Fc	2482.30	6318.65	31783.70	138245.10	2456.20	10388.89
Day 1	Placebo	38955.70	6426.96	65730.80	110671.70	5943.50	6100.67
Day 2	Placebo	29482.30	7060.88	93207.00	138453.90	8329.50	10360.84
Day 4	Placebo	59806.20	9786.00	110978.70	82253.30	16021.25	16711.52
Day 1	CD24Fc	17690.90	8616.95	73330.30	109931.60	10248.99	18538.14
Day 2	CD24Fc	8502.80	6484.37	54019.10	125514.50	7023.84	10738.17
Day 4	CD24Fc	23089.70	8607.59	89766.70	177149.00	8479.57	14029.47
Day 1	Placebo	10164.80	5447.75	112901.10	109930.20	11854.77	12375.65
Day 2	Placebo	14858.70	4730.92	97197.10	171049.80	14142.50	14675.06
Day 4	Placebo	8978.20	5663.67	113349.20	177335.70	15238.96	13485.05
Day 8	Placebo	16956.90	8116.78	110608.40	230518.80	8167.71	9987.45
Day 1	Placebo	14932.40	7820.00	84977.60	301168.80	12279.64	13920.26
Day 2	Placebo	9062.90	5993.27	98546.10	246127.00	11834.52	14630.67
Day 4	Placebo	6583.80	4159.20	126443.30	162871.40	12864.00	15020.67
Day 8	Placebo	3080.10	1648.78	119555.50	254994.60	12156.74	13396.67
Day15	Placebo	3636.70	3457.41	125005.80	191958.80	12072.96	17847.34
Day 1	Placebo	11103.50	4980.53	49911.60	197266.10	1765.74	12533.47
Day 2	Placebo	28342.70	7828.95	100563.20	235727.00	1940.20	9816.69
	Healthy Donors	3960.89	6085.31	38240.32	17368.84	2493.56	10451.86
	Healthy Donors	3381.81	4688.41	29705.19	93543.41	993.51	10128.32
	Healthy Donors	8761.60	6255.91	70391.10	68938.17	3619.28	14003.77
	Healthy Donors	13508.09	4992.83	65498.19	132306.88	3194.82	12013.94
	Healthy Donors	9198.63	3737.55	5900.02	8019.74	1724.98	9923.60
	Healthy Donors	21105.37	6468.69	7565.07	20337.87	1327.34	12997.18
	Healthy Donors	2949.02	4210.47	3998.44	3578.76	413.50	8806.99
	Healthy Donors	11620.35	5414.32	5080.38	12263.26	1675.20	19996.01
	Healthy Donors	4968.79	7055.69	4321.89	13786.96	612.64	10638.58
	Healthy Donors	22304.68	5759.16	3402.41	18092.45	938.61	13702.25
	Healthy Donors	28608.20	5128.12	7229.69	16793.00	1537.08	10663.17
	Healthy Donors	17908.57	8664.60	4440.02	16821.48	828.61	9714.93
	Healthy Donors	8798.81	8565.46	13761.00	25174.50	2790.58	19139.29
	Healthy Donors	2300.38	3043.60	4670.48	23555.51	500.16	13407.24

Time point	Treatment	Platelet- Derived Growth Factor-BB (PDGF-BB)	C-C Motif Chemokine Ligand 5 (CCL5; RANTES)	Tissue Inhibitor Of Metallo-proteinases-1 (TIMP-1)	Tissue Inhibitor Of Metallo-proteinases-2 (TIMP-2)	Tumor Necrosis Factor Receptor Superfamily, Member 1A (TNFRSF1A; TNF RI)	Tumor Necrosis Factor Receptor Superfamily, Member 1B (TNFRSF1B; TNF RII)
	Healthy Donors	54.03	2074.96	2605.46	16415.52	360.17	7992.47
	Healthy Donors	1414.00	1264.90	4050.64	27568.99	2030.96	11209.36
	Healthy Donors	1505.60	2550.17	6071.31	19949.35	775.19	12858.78
	Healthy Donors	5139.06	2664.92	9992.37	32729.47	753.52	15275.87
	Healthy Donors	5205.05	3787.68	6995.33	52357.71	2063.17	14296.43
	Healthy Donors	5618.89	2003.56	3942.30	22217.61	763.20	15905.40
	Healthy Donors	3239.22	4499.76	3787.37	25664.91	542.89	10306.04
	Healthy Donors	2100.41	4233.21	6606.73	9375.56	442.40	12187.09
	Healthy Donors	5131.01	2532.91	10255.04	31377.54	1377.20	11006.67
	Healthy Donors	8512.48	5040.65	11024.63	24748.87	2122.91	19722.80
	Healthy Donors	4864.90	2403.55	5014.03	31597.87	496.04	11622.77

Table S5. Centrality ranks of filtered and weighted correlations.

Cytokine markers	HD	D1	Placebo	CD24Fc	var	Mean
IL-5	1	1	1	9	16	3
MIP-1d	17	2	12	1	60·67	8
IL-1b	11	3	2	2	19	4·5
IL-8	2	4	8	17	44·25	7·75
G-CSF	20	5	9	4	53·67	9·5
IL-16	15	6	4	6	24·25	7·75
MIG	16	7	17	5	37·58	11·25
IL-4	10	8	6	3	8·92	6·75
MCSF	24	9	13	16	40·33	15·5
IL-12p40	14	10	5	7	15·33	9
IL-15	13	11	7	8	7·58	9·75
IL-1a	7	12	11	12	5·67	10·5
TNF RI	25	13	14	14	32·33	16·5
I-309	8	14	3	11	22	9
MIP-1a	12	15	21	13	16·25	15·25
BLC (CXCL13)	27	16	25	15	37·58	20·75
TNF RII	22	17	18	21	5·67	19·5
IL-6sR	30	18	28	22	30·33	24·5
IL-7	5	19	19	24	66·92	16·75
MIP-1b	19	20	27	30	28·67	24
IL-6	6	21	20	28	84·92	18·75
PDGF-BB	9	21	22	18	35	17·5
RANTES	18	23	23	19	6·92	20·75
GM-CSF	4	24	16	25	94·25	17·25
TIMP-1	23	25	24	20	4·67	23
IL-10	3	26	15	26	120·33	17·5
Eotaxin-2 (CCL24)	30	27	30	30	2·25	29·25
ICAM-1	30	28	26	23	8·92	26·75
Eotaxin (CCL11)	26	29	10	10	103·58	18·75
TIMP-2	21	30	29	27	16·25	26·75

HD, Healthy donor; D1, baseline COVID-19 patients; Var, variance.
Centrality scores ranked from highest (1, red) to lowest (30, blue). Variance and means calculated based on rank.

Table S6. Cytokine concentrations from plasma samples (pg/mL), as measured by Luminex.

Sample Description	time point	IFNγ	IL-1Ra	IL-2	IL-12p40	IL-13	MCP-1	TNFα
COVID-19 patient	D0	1.22	13.07	0	59.3	3.44	325.61	73.72
COVID-19 patient	D1	0.91	10.42	0	46.81	8.49	306.43	69.88
COVID-19 patient	D4	0.85	23.88	0.08	38.36	12.82	186.64	71.28
COVID-19 patient	D8	0.29	22.07	0	44	13.84	191.45	82.08
COVID-19 patient	D0	0.48	8.09	0	63.43	7.32	83.25	43.19
COVID-19 patient	D1	1.01	10.42	0.18	111.96	26.73	112.36	63.59
COVID-19 patient	D4	0.06	7.47	0	60.68	4.82	109.11	48.84
COVID-19 patient	D0	3.55	24.42	0.81	109.3	70.43	188.98	64.99
COVID-19 patient	D1	2.64	15.17	0.53	87.9	53.82	143.75	55.87
COVID-19 patient	D4	1.96	14.94	0.41	82.5	62.95	123.97	59.03
COVID-19 patient	D0	0.98	8.82	0.04	60.68	16.8	254.19	14.91
COVID-19 patient	D1	1.13	6.58	0.06	71.64	9.62	232.21	15.63
COVID-19 patient	D4	0.19	4.38	0	31.24	14.84	59.14	11.62
COVID-19 patient	D8	0.66	14.59	0.04	41.19	27.58	52.6	19.62
COVID-19 patient	D0	1.72	16.64	0.53	103.98	20.55	170.63	46.72
COVID-19 patient	D1	1.22	12.95	0.41	82.5	11.78	149.28	37.16
COVID-19 patient	D4	0.6	10.3	0.24	53.77	8.49	122.47	31.11
COVID-19 patient	D8	0.38	16.7	0.16	49.6	8.49	147.19	29.68
COVID-19 patient	D0	0.63	20.21	0	115.94	0	264.77	92.84
COVID-19 patient	D1	0.1	12.26	0	74.37	0	283.46	89.37
COVID-19 patient	D4	0.51	10.19	0.08	41.19	15.83	202.11	72.67
COVID-19 patient	D8	0.29	23.27	0.2	55.16	12.82	174.03	74.07
COVID-19 patient	D0	3.58	30.24	0.53	126.5	35.78	277.08	71.28
COVID-19 patient	D1	1.38	7.98	0.12	74.37	8.49	251.69	51.3
COVID-19 patient	D4	0	2.87	0	21.09	3.44	126.73	28.25
COVID-19 patient	D8	0	3.78	0	18.14	0	87.56	28.25
COVID-19 patient	D0	9.19	3.08	1.53	63.43	135.35	111.98	124.62
COVID-19 patient	D1	14.35	4.76	2.67	63.43	224.15	107.05	149.7
COVID-19 patient	D4	34.26	11.8	17.06	94.62	517.04	116.87	403.53
COVID-19 patient	D0	0.85	4.54	0.16	44	17.76	172.2	22.87
COVID-19 patient	D1	0.6	4	0.12	53.77	23.25	155.38	30.4
COVID-19 patient	D4	0.38	5.14	0	41.19	12.82	156.21	27.54
COVID-19 patient	D0	1.16	6.86	0.04	44	0	275.64	67.08
COVID-19 patient	D1	0.22	3.94	0	26.92	0	86.91	28.97
COVID-19 patient	D4	0.1	3.3	0	12.15	0	157.46	37.87
COVID-19 patient	D8	0.03	2.39	0	26.92	0	249.52	43.19
COVID-19 patient	D0	2.06	15.52	0	59.3	24.13	140.6	23.23
COVID-19 patient	D1	0.73	16.52	0.04	44	12.82	74.46	12.35
COVID-19 patient	D4	1.87	27.65	0.12	32.67	32.57	89.11	16.72
COVID-19 patient	D0	0.54	1.31	0	46.81	13.84	118.75	16.72
COVID-19 patient	D1	0.35	1.82	0	32.67	10.71	105.57	22.15
COVID-19 patient	D4	0.22	1.82	0	15.16	3.44	114.43	24.67
COVID-19 patient	D0	1.07	10.53	0.49	56.54	6.11	389.01	62.19
COVID-19 patient	D1	0.22	4.98	0.08	29.8	0	247.09	28.97

COVID-19 patient	D4	0.73	6.86	0.75	44	18.7	204.55	38.94
COVID-19 patient	D0	27.23	38.71	15.52	127.82	42.01	417.7	13.81
COVID-19 patient	D1	22.24	28.76	15.2	105.31	43.53	392.58	17.09
COVID-19 patient	D4	9.25	13.24	4.35	42.6	22.36	199.27	9.41
COVID-19 patient	D0	0.41	11.68	0.92	45.4	9.62	260.8	17.09
COVID-19 patient	D1	0.45	9.28	0.88	38.36	12.82	166.17	6.07
COVID-19 patient	D4	0.98	17.59	2.2	66.17	6.11	236.62	11.98
COVID-19 patient	D0	1.16	2.13	0	4.36	37.36	147.73	21.79
COVID-19 patient	D1	0.29	2.29	0	0	17.76	138.1	13.08
COVID-19 patient	D0	0.29	1.82	0	2.72	0	187.44	11.62
COVID-19 patient	D1	9.9	30.48	5.67	68.91	6.11	76.4	21.43
COVID-19 patient	D4	12.32	56.02	9.1	74.37	3.44	81.84	27.89
COVID-19 patient	D15	2.58	25.09	0.66	59.3	4.82	200.28	33.25
COVID-19 patient	D0	236.42	759.93	289.29	10882.88	1943.64	463.22	1704.05
COVID-19 patient	D1	347.46	1199.21	461.36	16632.73	3065.34	454.3	3334.43
COVID-19 patient	D4	198.99	596.02	235.94	8947.27	1657.59	221.17	1668.81
COVID-19 patient	D0	2.61	11.22	1.55	26.92	12.82	236.42	28.97
COVID-19 patient	D1	35.76	75.5	61.75	32.67	14.84	112	18.18
COVID-19 patient	D4	108.81	197.52	145.81	79.79	17.76	189.04	25.03
COVID-19 patient	D0	1.53	16.41	0.88	38.36	25.87	161.79	37.87
COVID-19 patient	D1	0.79	8.71	1.09	25.47	30.93	101.62	25.39
COVID-19 patient	D4	0.48	11.16	1.57	26.92	23.25	76.16	25.03
COVID-19 patient	D8	0.35	12.32	0.28	19.62	23.25	155.09	32.54
COVID-19 patient	D0	17.44	15.99	3.6	60.68	8.49	151.27	38.23
COVID-19 patient	D1	17.26	15.88	3.73	55.16	3.44	154.1	35.39
COVID-19 patient	D4	21.59	62.11	2.82	44	0	126.04	76.85
COVID-19 patient	D8	3.52	18.95	0.7	22.56	0	101.39	62.19
COVID-19 patient	D15	1.16	42.63	0.28	35.52	18.7	107.17	87.98
COVID-19 patient	D0	3.86	4.05	0	13.66	35.78	54.55	35.39
COVID-19 patient	D1	1.72	3.4	0	9.08	17.76	52.82	22.51
Non-COVID-19 control		0.41	2.03	0	53.77	0	145.24	28.25
Non-COVID-19 control		9.84	14.47	5.81	66.17	135.35	88.22	68.83
Non-COVID-19 control		0.29	1.51	0	49.6	8.49	165.32	13.81
Non-COVID-19 control		0.1	6.13	0	24.02	3.44	180.28	19.62
Non-COVID-19 control		1.72	9.33	0.62	98.63	48.01	188.74	45.31
Non-COVID-19 control		3.58	53.93	10.46	101.31	8.49	134.04	21.07
Non-COVID-19 control		1.84	6.47	0.18	75.72	46.52	182.06	44.95
Non-COVID-19 control		0.79	12.14	0.14	29.8	16.8	103.61	25.39
Non-COVID-19 control		0.32	1.21	0	60.68	17.76	90.34	5.69
Non-COVID-19 control		1.04	21.05	1.8	41.19	15.83	92.5	12.35
Non-COVID-19 control		0.6	12.38	0	91.93	29.27	130.64	16
Non-COVID-19 control		3.64	27.35	1.22	85.2	30.93	159.25	32.54
Non-COVID-19 control		2.82	5.69	0.7	156.61	88.65	107.47	69.88
Non-COVID-19 control		5.76	9.39	3.75	85.2	103.55	124.05	62.19
Non-COVID-19 control		6.12	2.13	3.21	111.96	146.1	132.05	85.9
Non-COVID-19 control		1.41	5.19	0.62	77.08	62.26	59.27	21.07
Non-COVID-19 control		17.73	34.83	16.38	447.81	312.91	101.56	187

Non-COVID-19 control	0.48	2.13	0	87.9	4.82	131.76	4.19
Non-COVID-19 control	0.41	3.73	0	220.97	6.11	86.95	46.01
Non-COVID-19 control	0.41	2.34	0	97.3	8.49	263.48	41.77
Non-COVID-19 control	0.48	1.31	0	21.09	0	147.42	19.26
Non-COVID-19 control	4.67	111.57	8.06	265.35	168.68	286.82	51.65
Non-COVID-19 control	156.21	98.79	44.13	677.79	2529.18	213.04	1020.33